Long-Range Diffusion- and Interface Reaction-Controlled Migration of Ferrite/Austenite Boundaries During Austenitization of Iron Alloys

Eric Schmidt
Sridhar Seetharaman
Carnegie Mellon University
Dept. of Materials Science and Engineering
Pittsburgh, PA

ALEMI
June 18-19
McMaster University
Hamilton, ON

Outline

- Introduction
  - Thermal processing of steel
- Previous results:
    - Austenite formation in pure iron/IF steel
    - austenite formation in alloy steel
- Objective
- Approach
- New Results and Analysis: Binary Fe-C
  - Austenite formation under non-isothermal conditions
  - Austenite formation under isothermal conditions
- Summary
  - Future Goals
- Acknowledgements
- Discussion

Thermal Processing of Steel

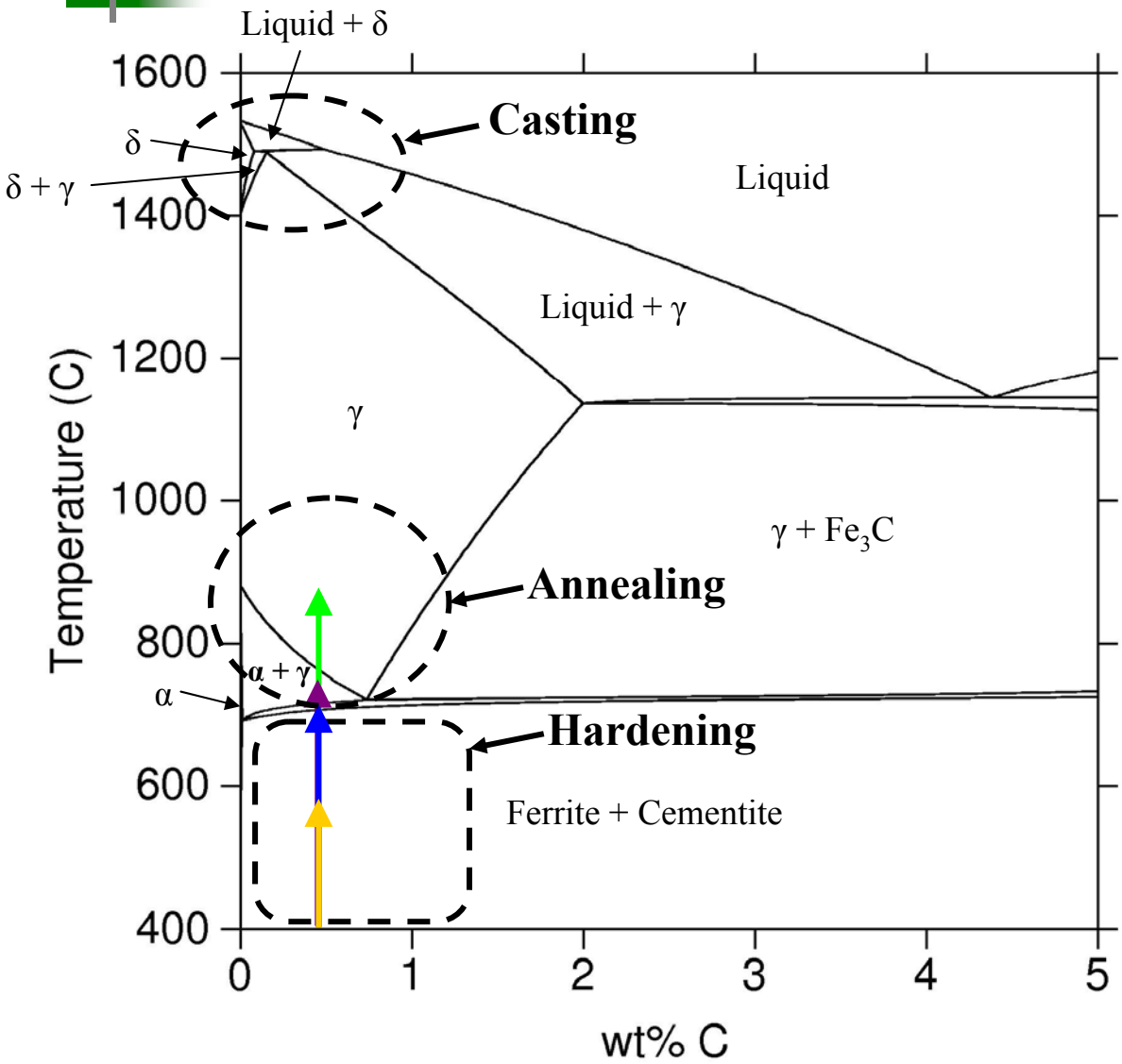

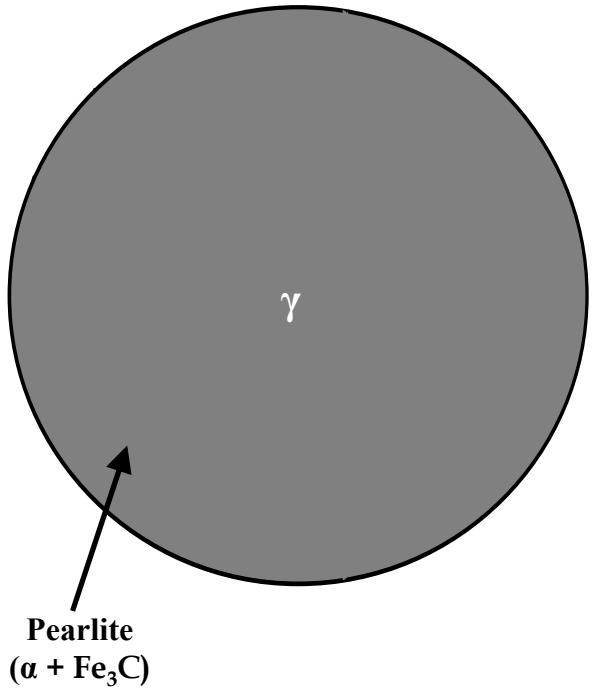

Austenitization in IF Steel

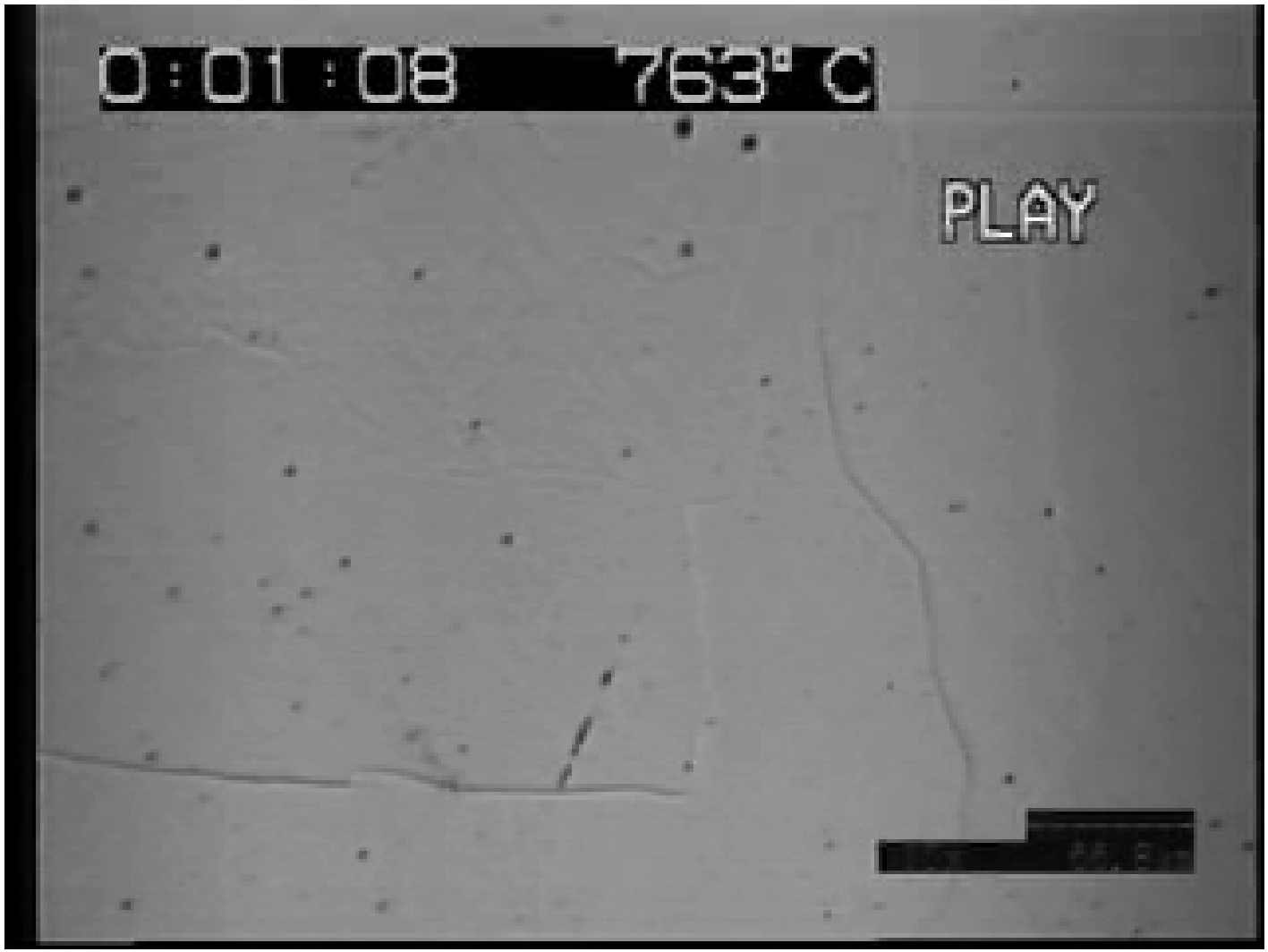

IF-A, 10 K/s constant heating rate

Austenitization Kinetics in Pure Iron and IF Steel

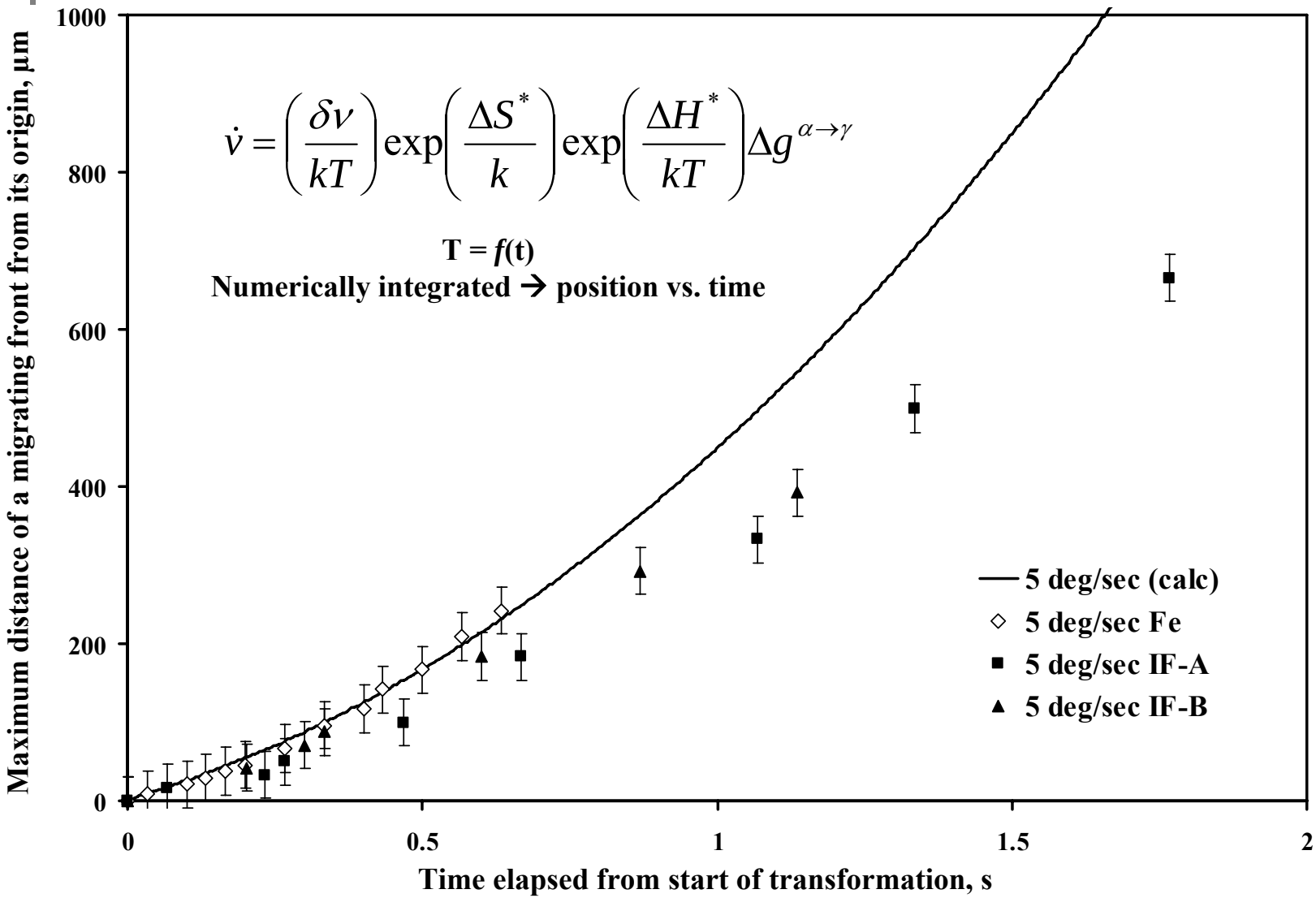

Austenitization Kinetics in Alloy Steel

- Migration kinetics appear to be:
  - long-range diffusion-controlled in the intercritical region below T_0
  - interface reaction-controlled above T_0

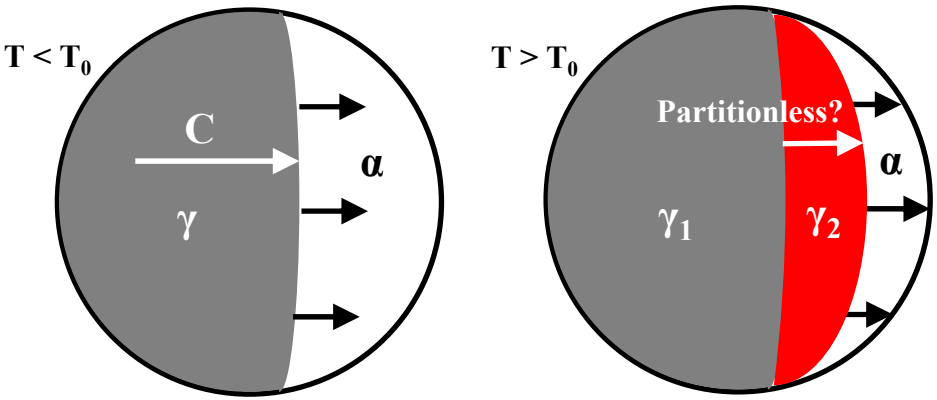

- Transition is difficult to isolate because:
  - Alloys have complicated thermodynamics
    - Para-equilibrium assumption may not be valid
  - Microstructure is not uniform

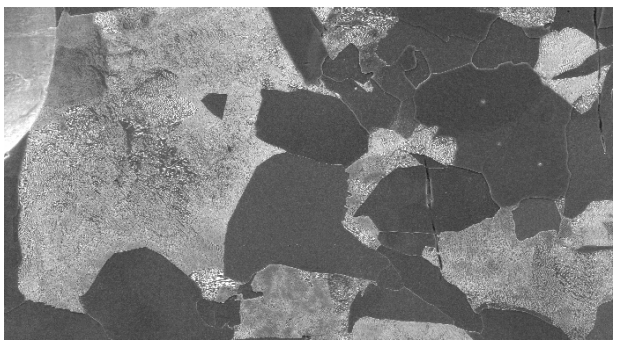

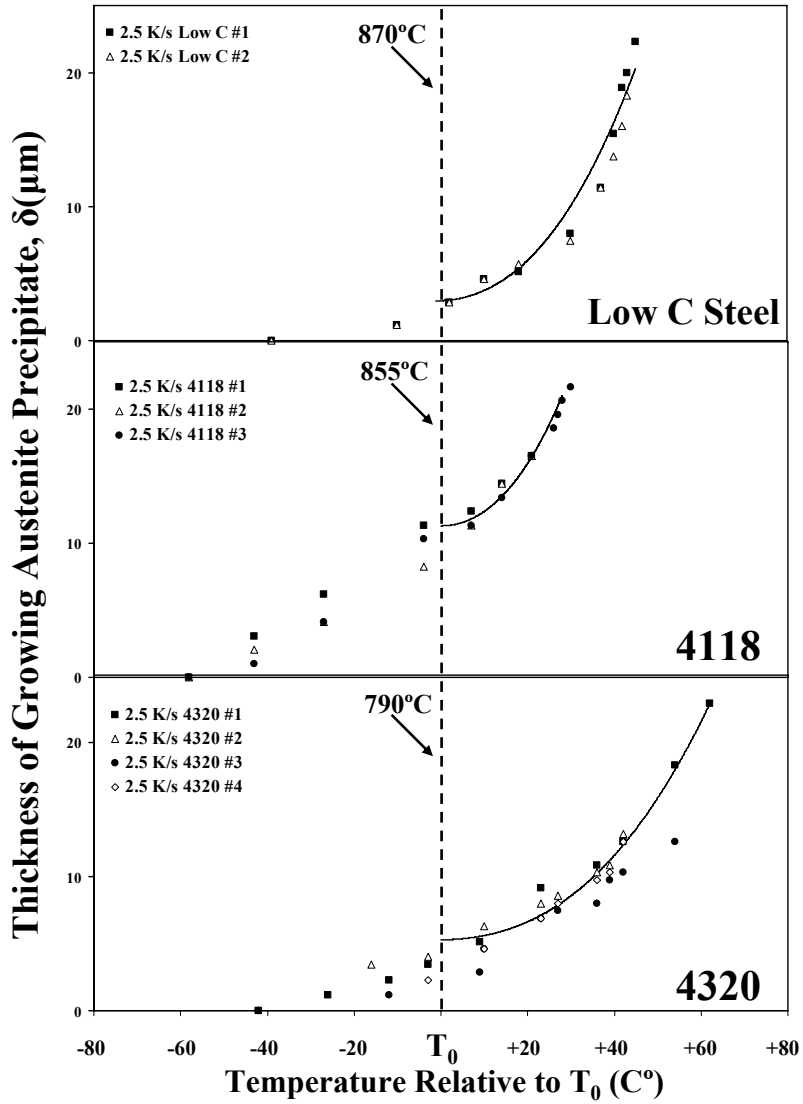

Characteristics of a Massive Transformation

- Will only occur above T_0 for any alloy
  - Generally observed above Ac_3
- Kinetics controlled by processes at the interface
- No homogenization of carbon
  - Previous investigation of 4118 alloy indicates that this may occur during austenitization when heating above T_0

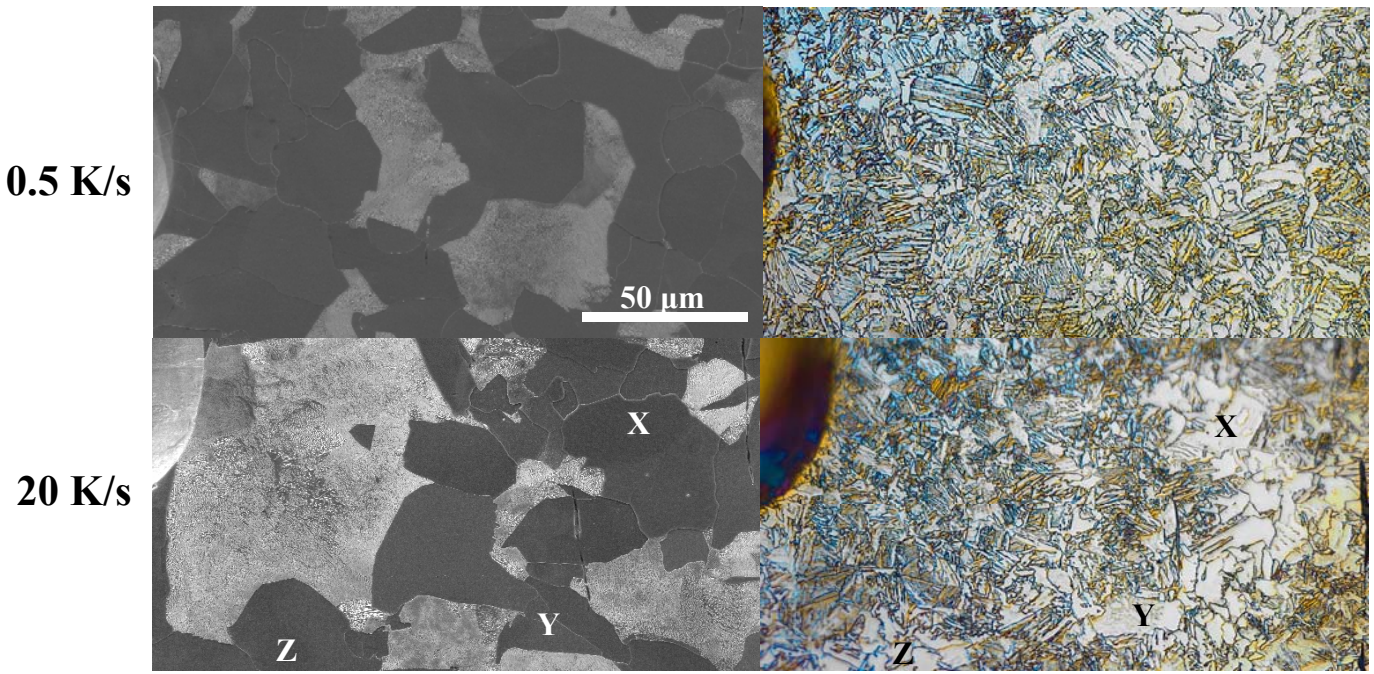

Objectives

- Observe austenitization in a binary Fe-C alloy
  - Fewer thermodynamic variables will improve the accuracy of model calculations
- Use finite difference technique to model diffusion controlled growth
  - Accounts for variations in size in the initial microstructure
- Compare observations within the region where both diffusion- and interface reaction-controlled boundary migration can occur
  - When/how can this transformation occur?
- Compare interface-controlled migration in Fe-C with previous studies for iron and alloy steels
  - What is the effect of carbon on mobility?

Approach: CSLM

- High Temperature Confocal Scanning Laser Microscopy

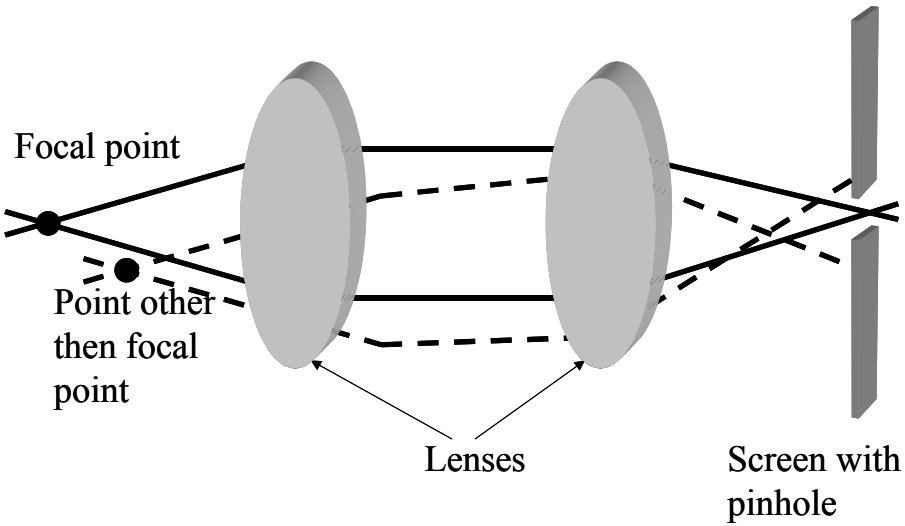

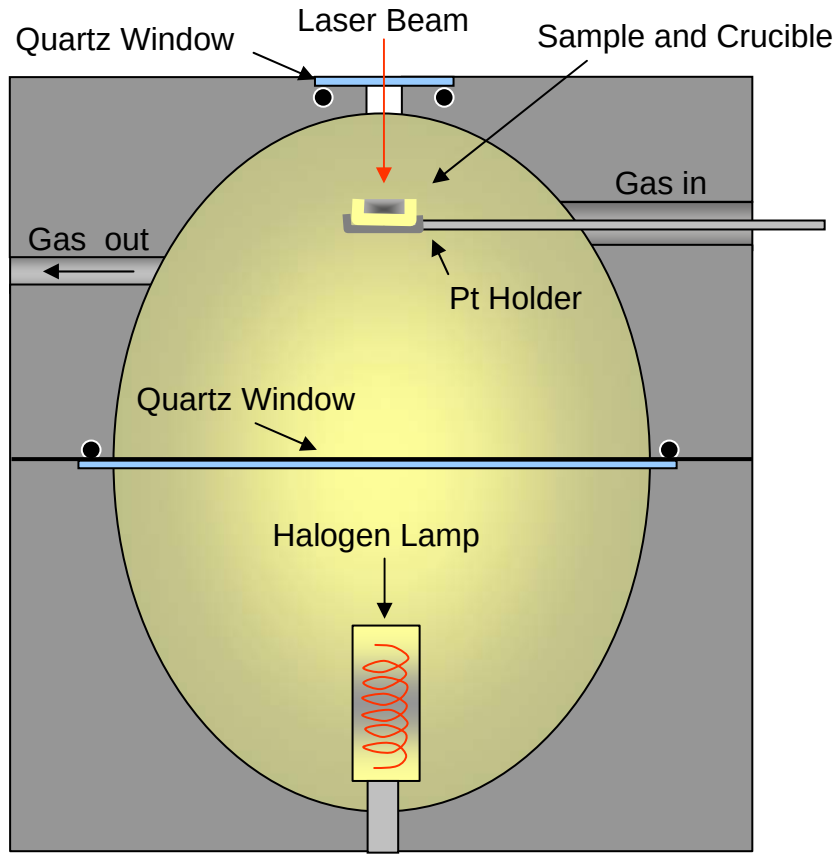

Approach: Procedure

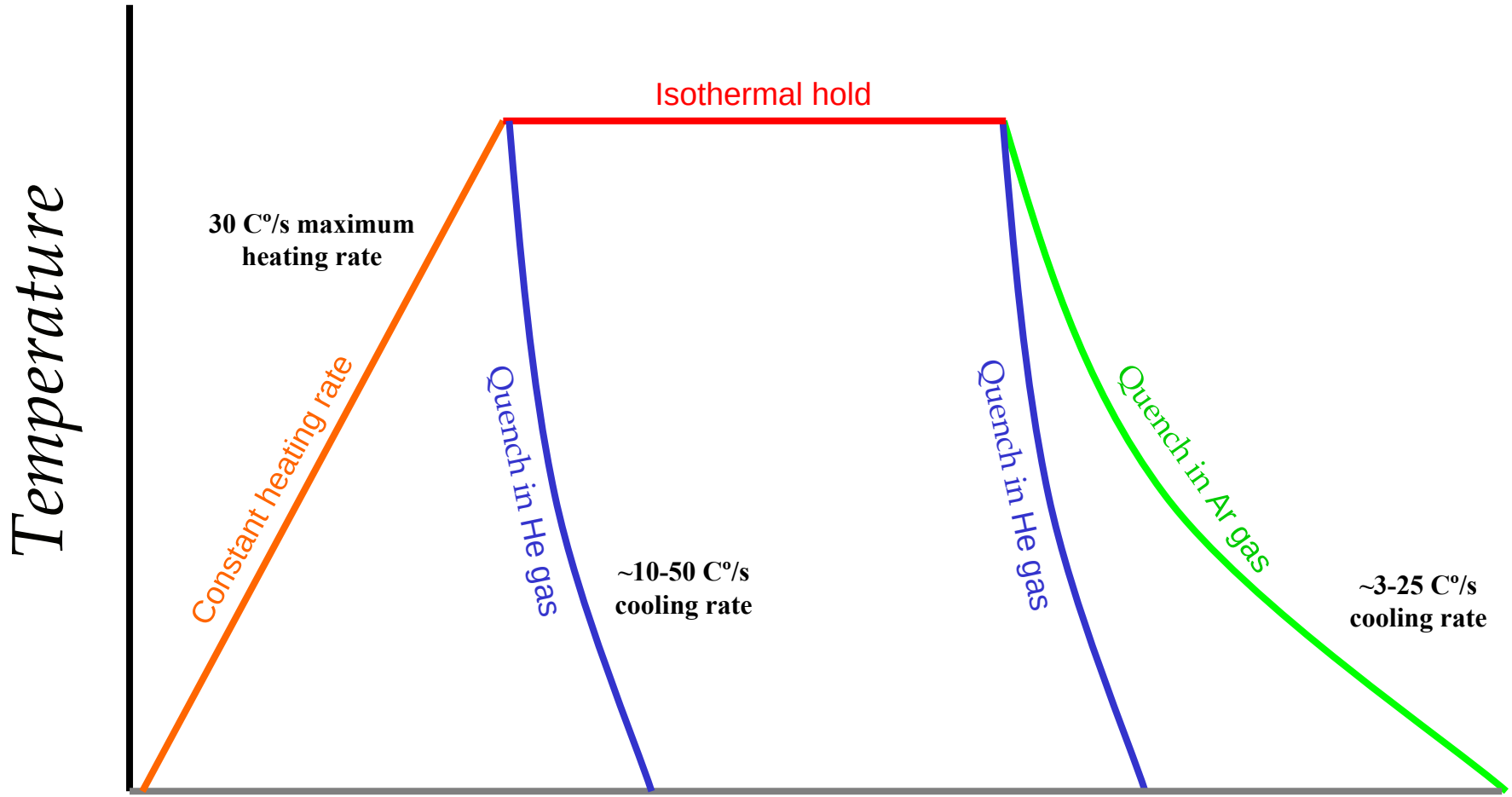

Starting structure for studying transformation during heating or under isothermal conditions

Fe-C During Heating

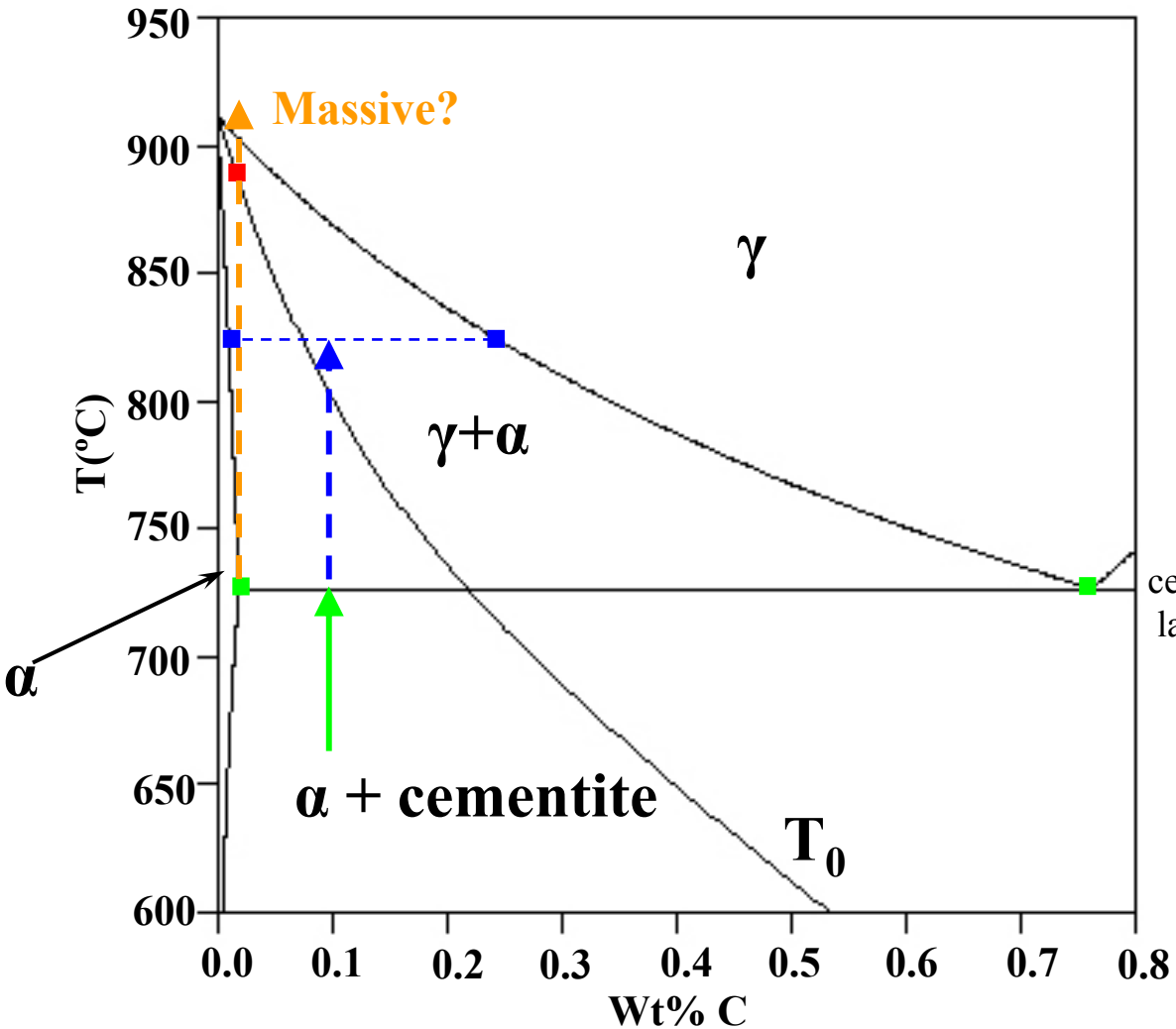

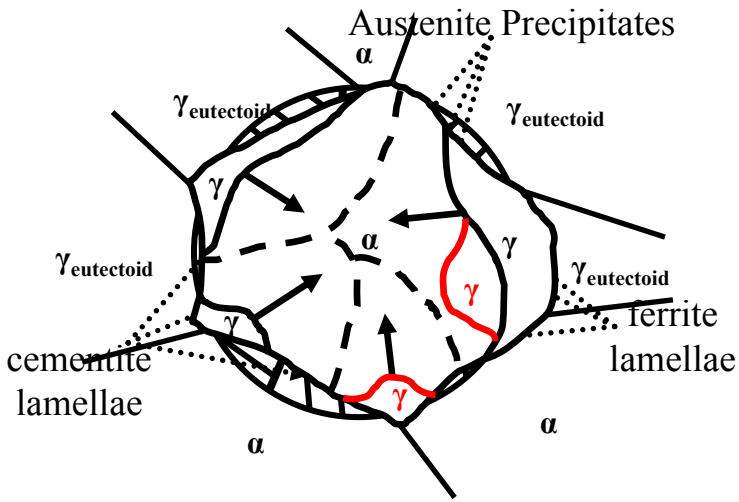

Observations: Normalized Fe-C

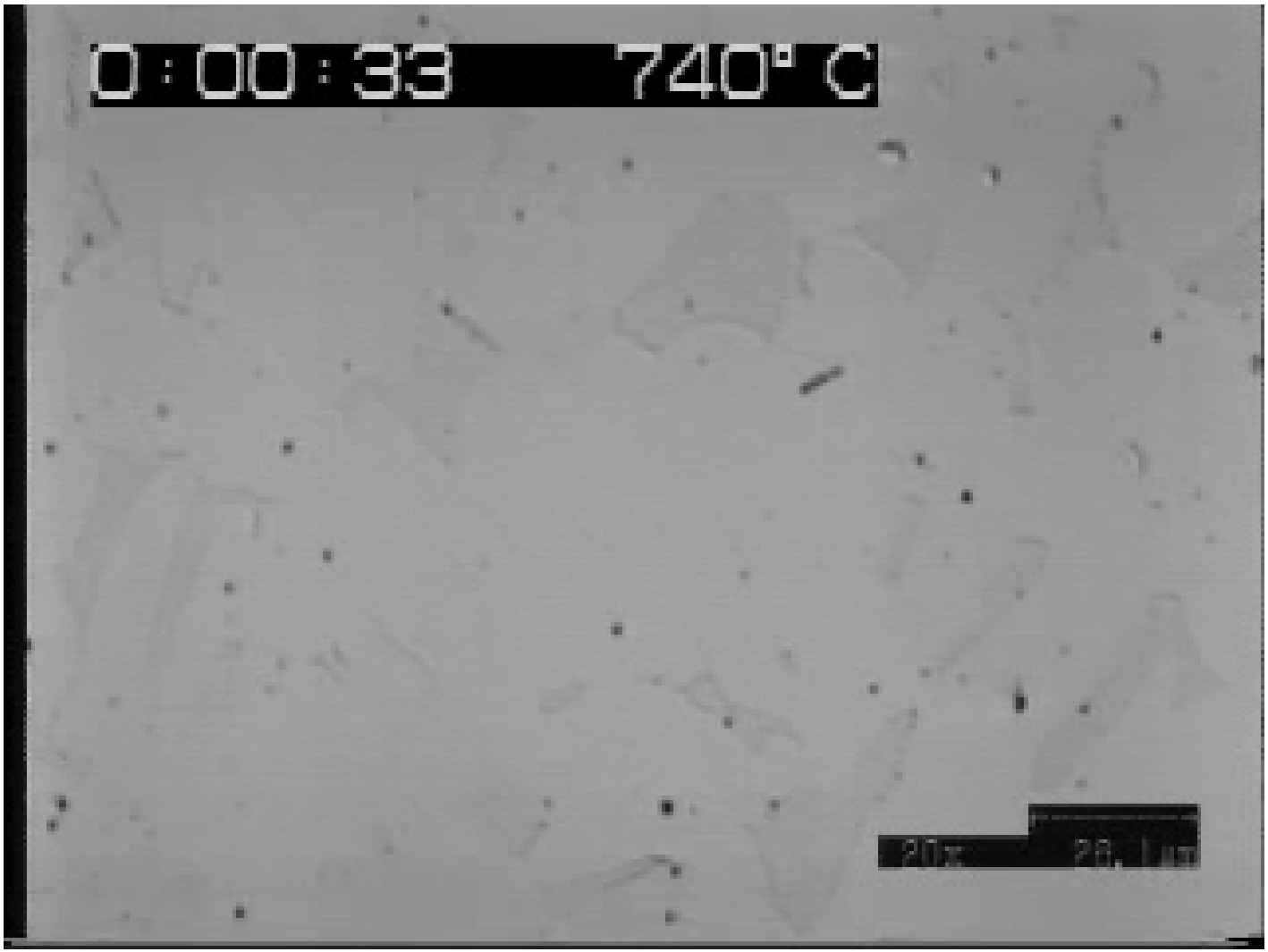

- 20 K/s heating
- 900°C isothermal

Migration Patterns and Trends: Mixed Microstructure

- In ferrite/carbide aggregates:

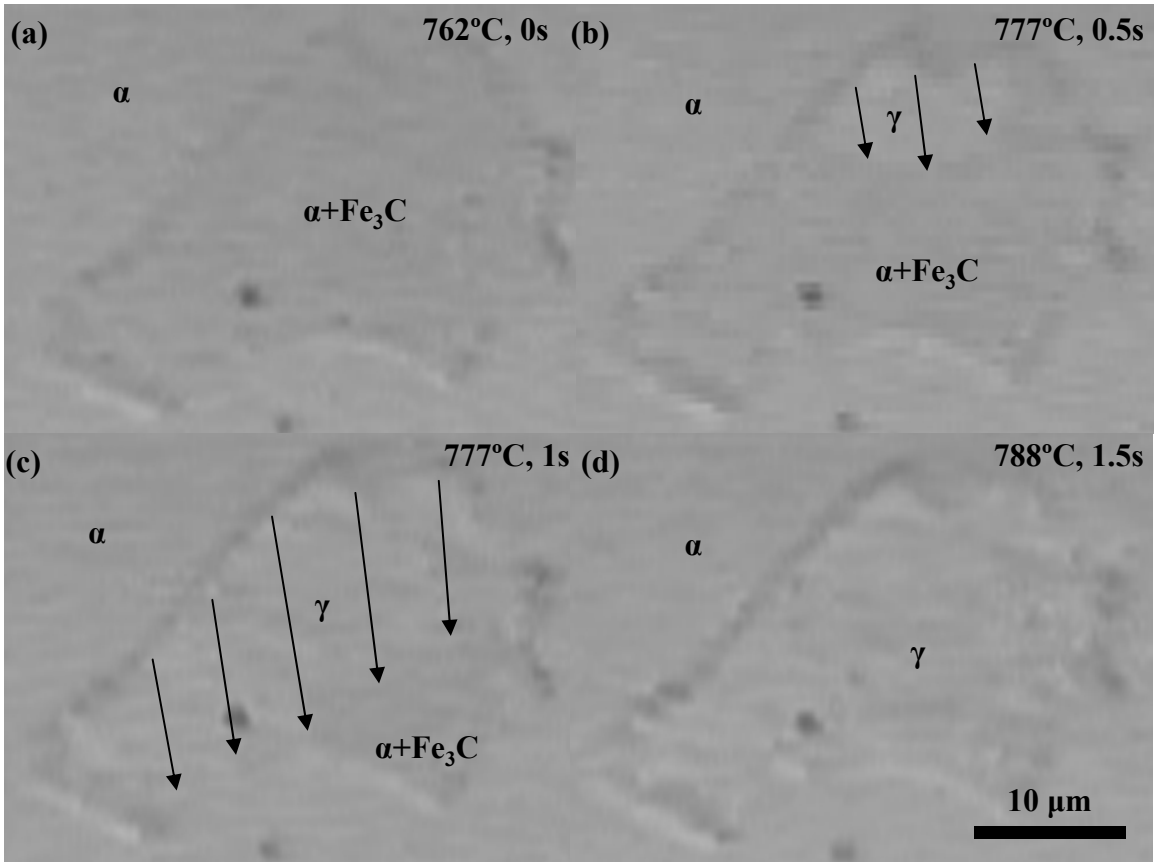

- Singe front
- Shape is maintained
- Easily discernable when all lamella within a pearlite region are oriented in a relatively uniform direction
- In these cases the migration follows the lamella

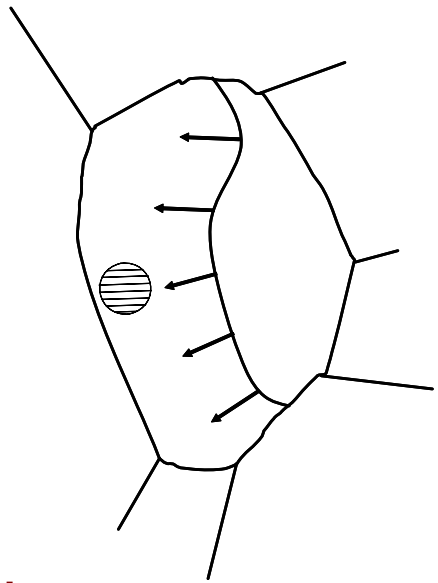

Migration Patterns and Trends: Mixed Microstructure

- In ferrite:

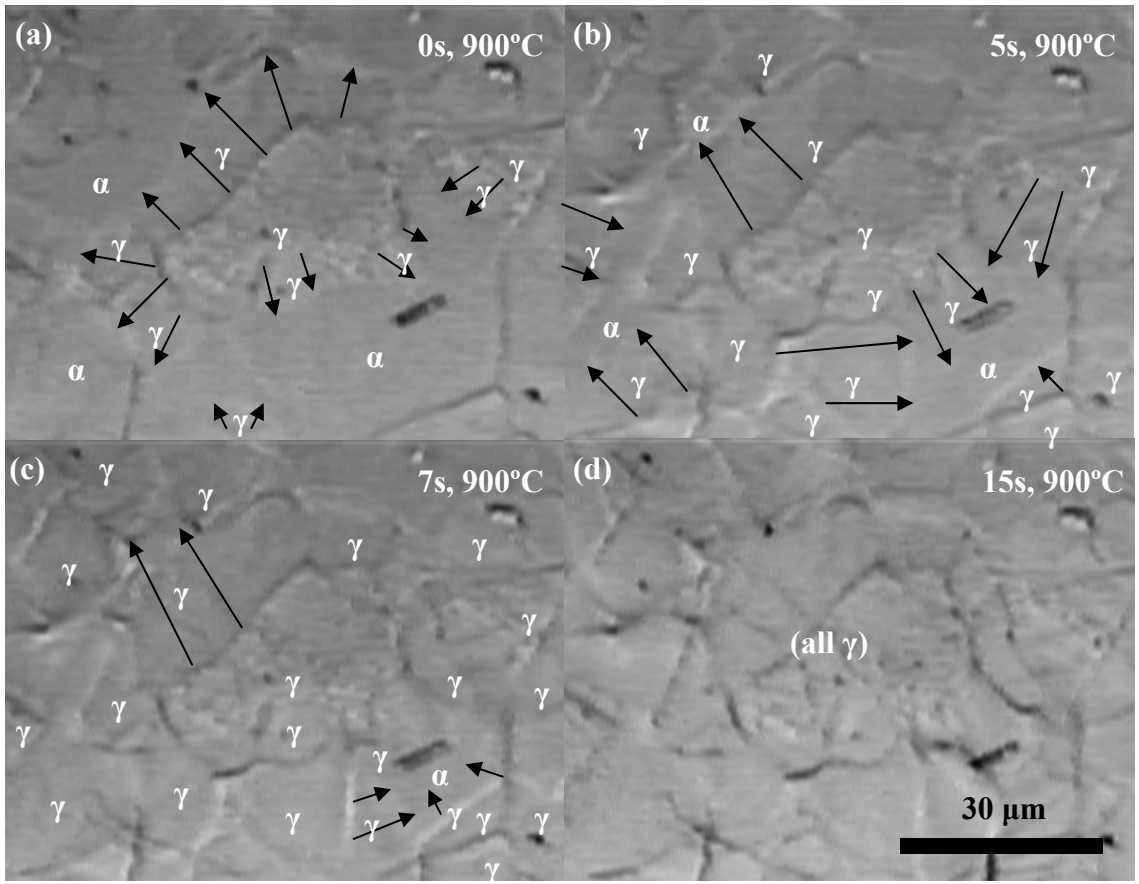

- Multiple fronts/perturbations
- Smooth interface
- Front shape is maintained
- Red fronts only appear at higher temperatures

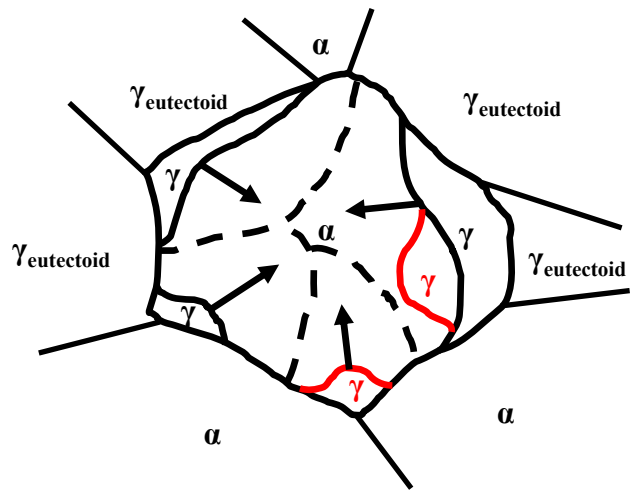

Fe-C: Non-Isothermal Results

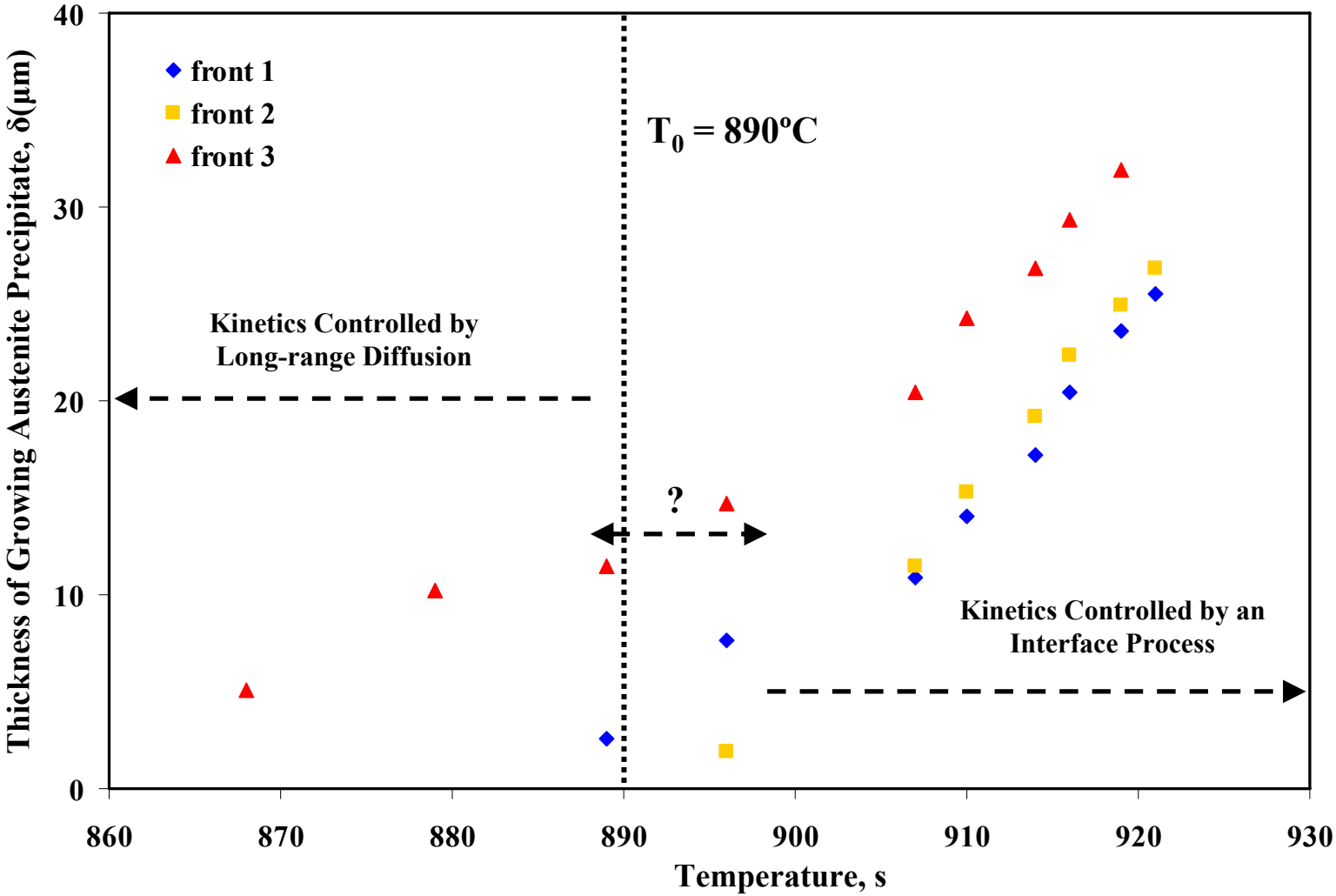

Fe-C: Isothermal Results

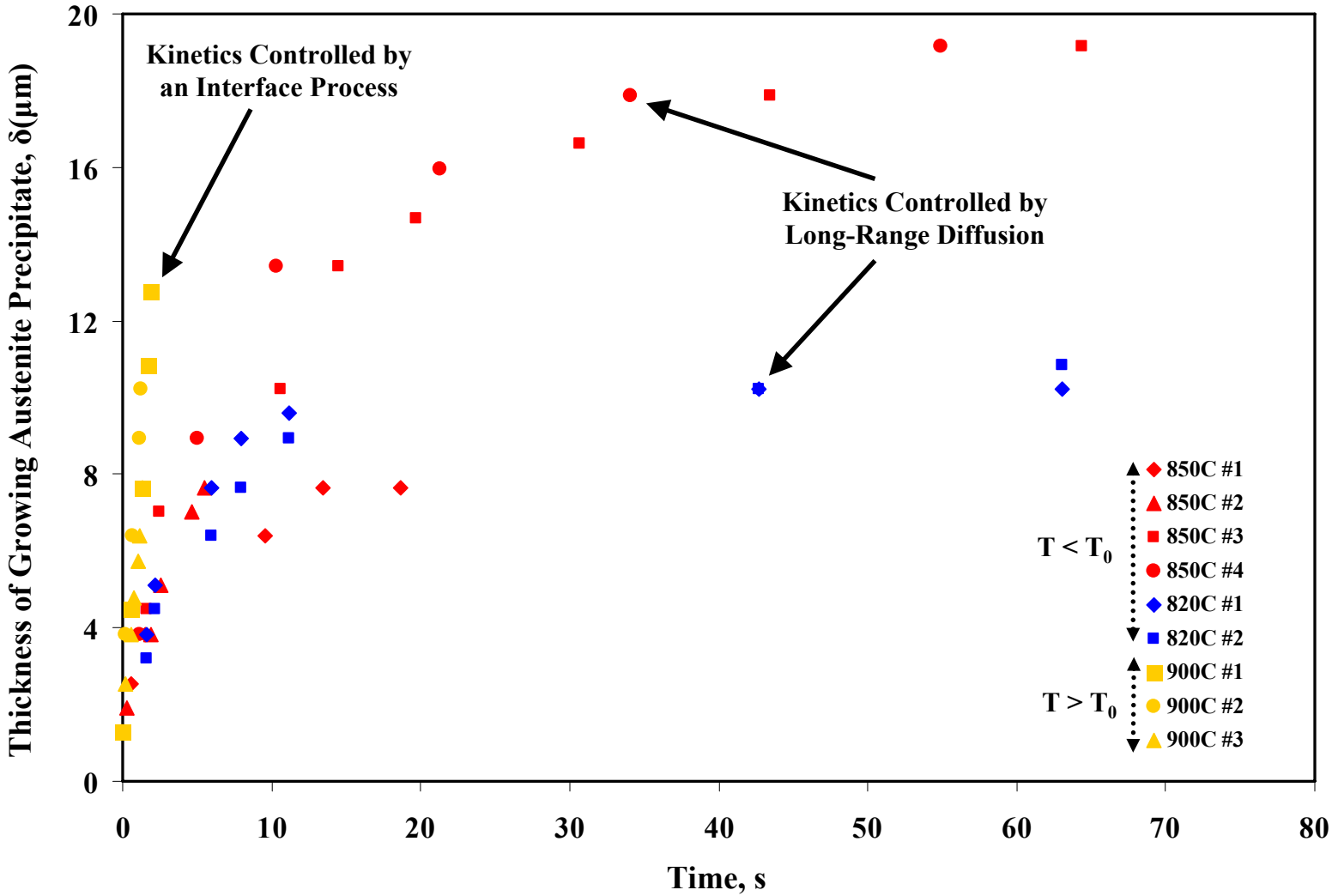

Long-Range Diffusion Controlled Interface Migration

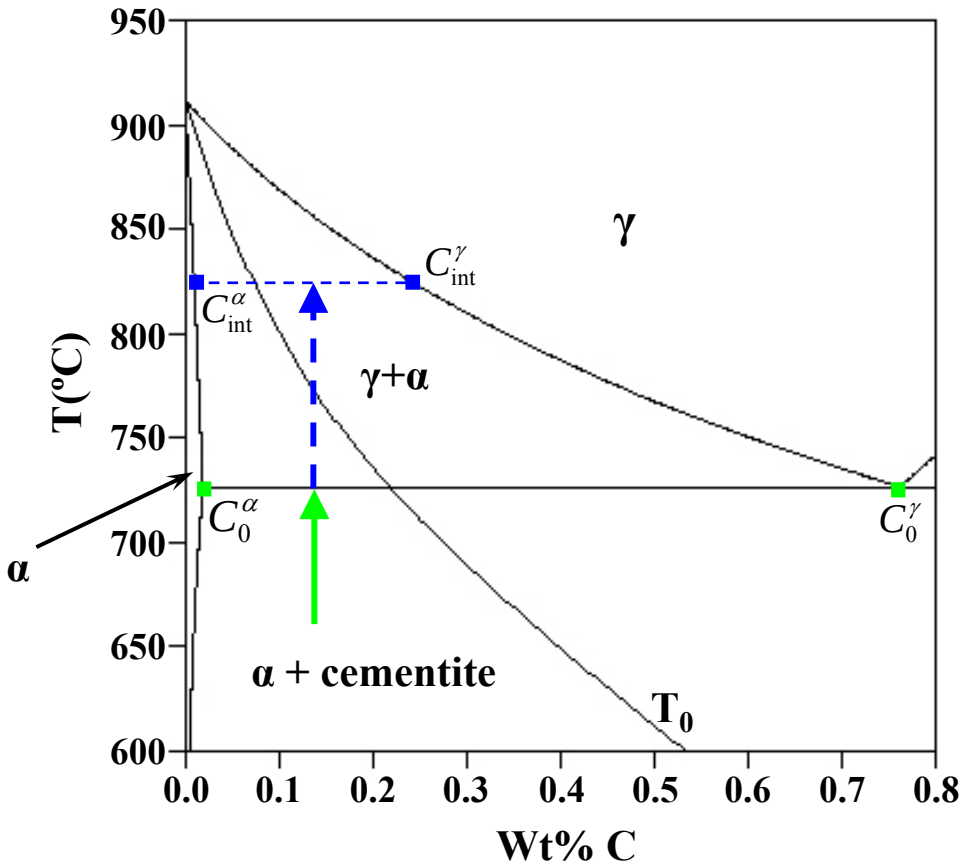

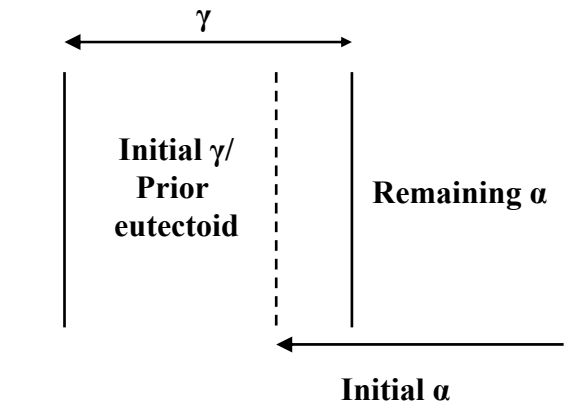

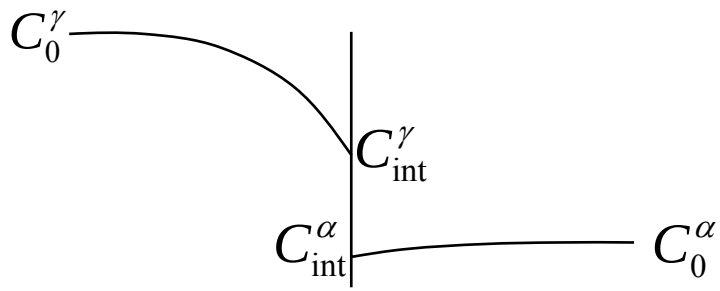

- Note: T_0 not valid for bulk composition during heating

Diffusion Controlled Growth: Finite Difference Model

- Following Sekerka and Wang, 1999
- Assume planar boundary (1-D)
- Express Fick's Second Law as a difference equation:

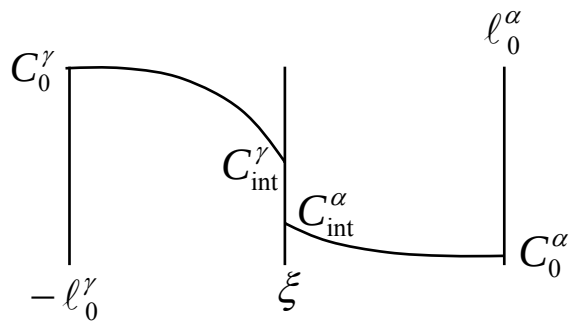

$$\frac{c_{i+1,j}-c_{i,j}}{\Delta t} = D\frac{c_{i,j+1}-2c_{i,j}+c_{i,j-1}}{(\Delta x)^2}$$

- Moving boundary requires expanding and contracting coordinates:

$$\Delta x_i^\alpha = \frac{\left(\ell_0^\alpha - \xi_i\right)}{N^\alpha} \qquad \Delta x_i^\gamma = \frac{\left(\ell_0^\gamma + \xi_i\right)}{N^\gamma}$$

- Use the following diffusion equations:

$$\left(c_{i,0}^\gamma - c_{i,0}^\alpha\right)\left(\frac{\xi_{i+1}-\xi_i}{\Delta t}\right) = -D^\gamma\frac{c_{i,0}^\gamma - c_{i,-1}^\gamma}{\Delta x_i^\gamma} + D^\alpha\frac{c_{i,1}^\alpha - c_{i,0}^\alpha}{\Delta x_i^\alpha}$$

is solved from the initial concentration to determine the boundary movement, and the result can be used to determine the new concentration profile (and new grid spacings):

$$\frac{c_{i+1,j}^\gamma - c_{i,j}^\gamma}{\Delta t} = \frac{c_{i,j+1}^\gamma - c_{i,j-1}^\gamma}{2\Delta x_i^\gamma}\left(\frac{N^\gamma + j}{N^\gamma}\right)\left(\frac{\xi_{i+1}-\xi_i}{\Delta t}\right) + D^\gamma\frac{c_{i,j+1}^\gamma - c_{i,j}^\gamma + c_{i,j-1}^\gamma}{\left(\Delta x_i^\gamma\right)^2}$$

$$\frac{c_{i+1,j}^\alpha - c_{i,j}^\alpha}{\Delta t} = \frac{c_{i,j+1}^\alpha - c_{i,j-1}^\alpha}{2\Delta x_i^\alpha}\left(\frac{N^\alpha + j}{N^\alpha}\right)\left(\frac{\xi_{i+1}-\xi_i}{\Delta t}\right) + D^\gamma\frac{c_{i,j+1}^\alpha - c_{i,j}^\alpha + c_{i,j-1}^\alpha}{\left(\Delta x_i^\alpha\right)^2}$$

Isothermal Results vs. FDM: Fe-C, 850°C

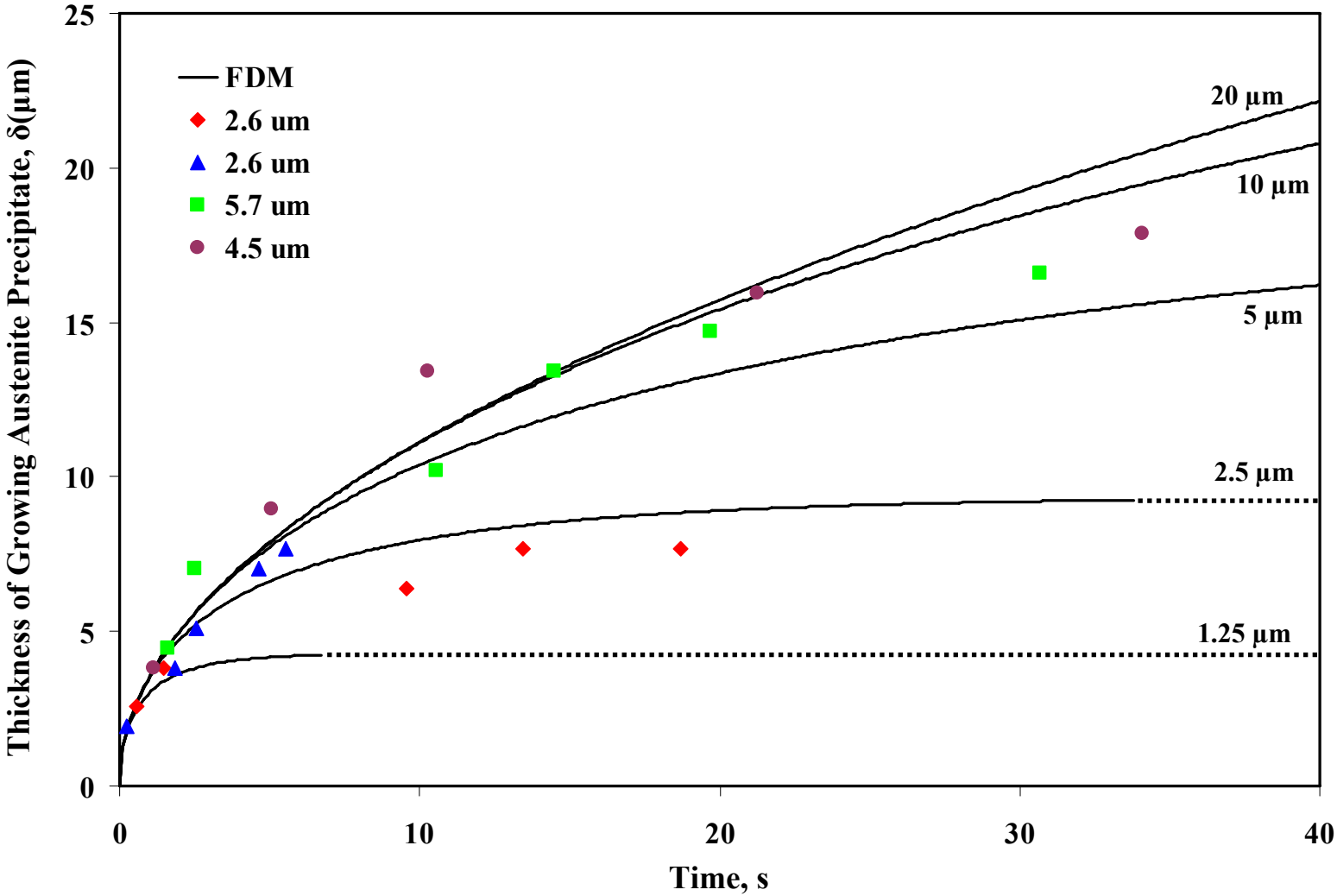

Isothermal Results vs. FDM: 810°C, 4118

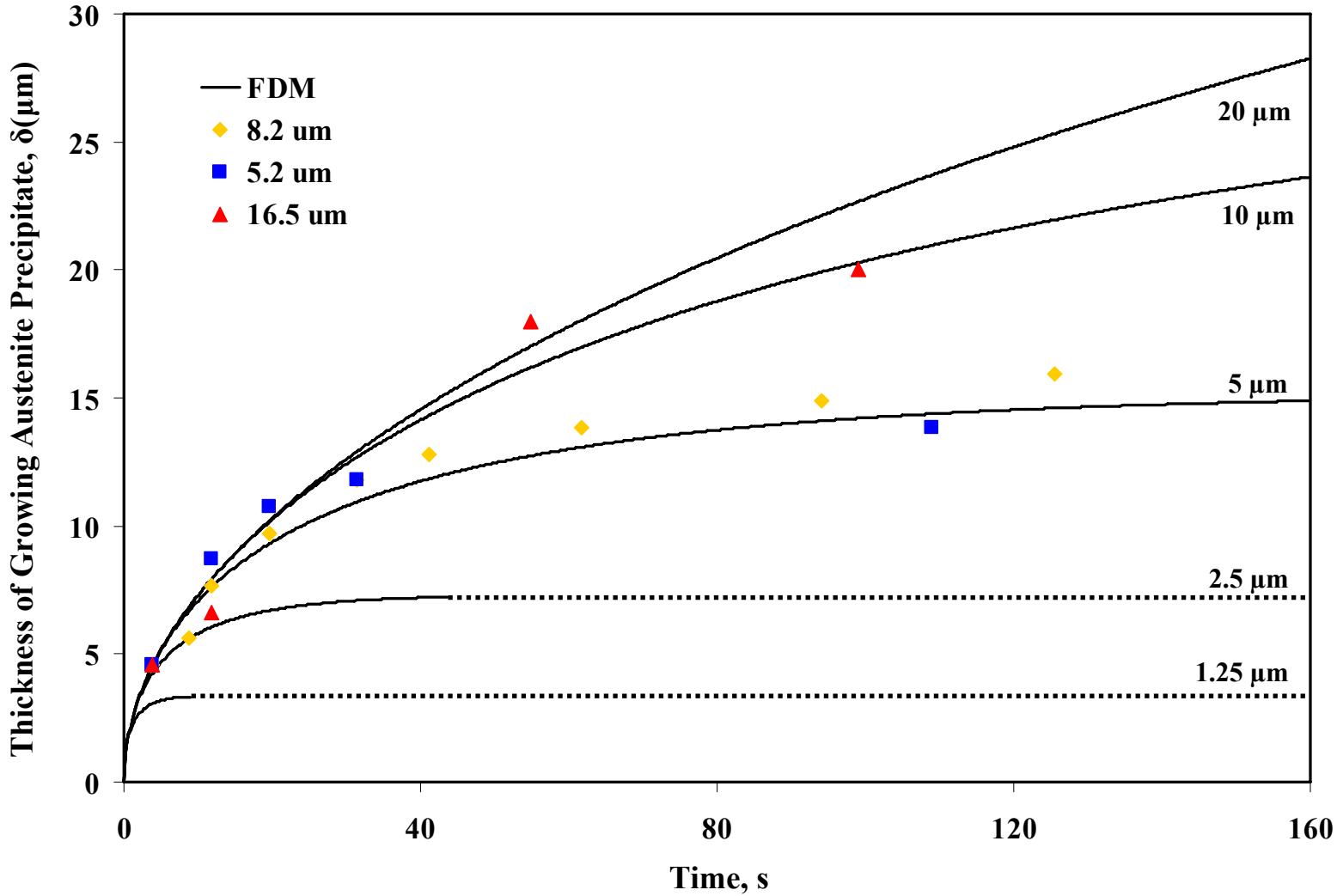

Interface Reaction-Controlled Interface Migration

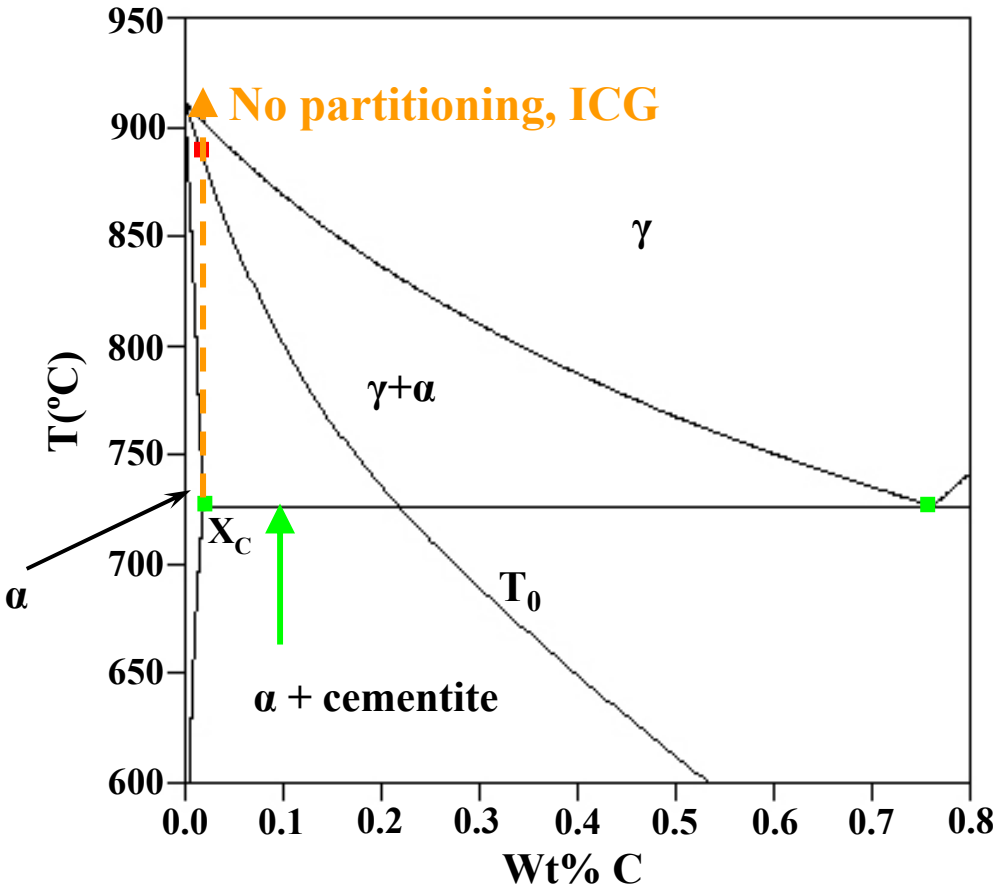

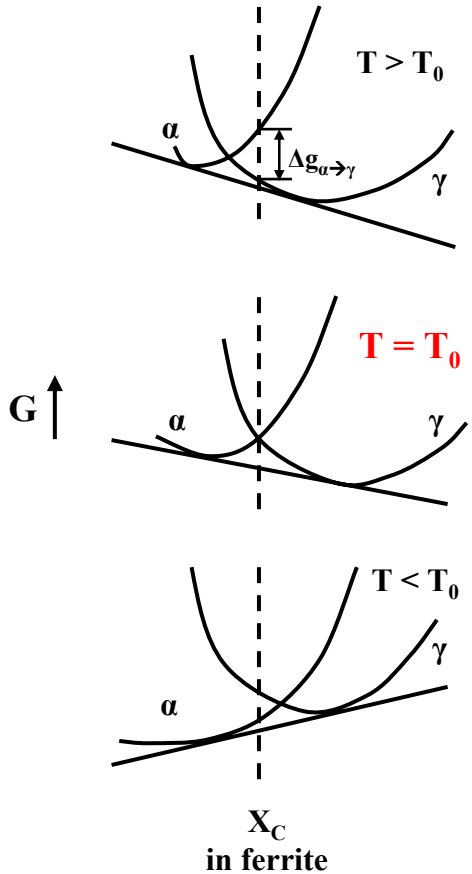

$$v = \left(\frac{\delta\nu}{kT}\right)\exp\left(\frac{\Delta S^*}{k}\right)\exp\left(\frac{\Delta H^*}{kT}\right)\Delta g^{\alpha\rightarrow\gamma}$$

Uncorrelated atom jumping across interface

Interface Reaction Kinetics

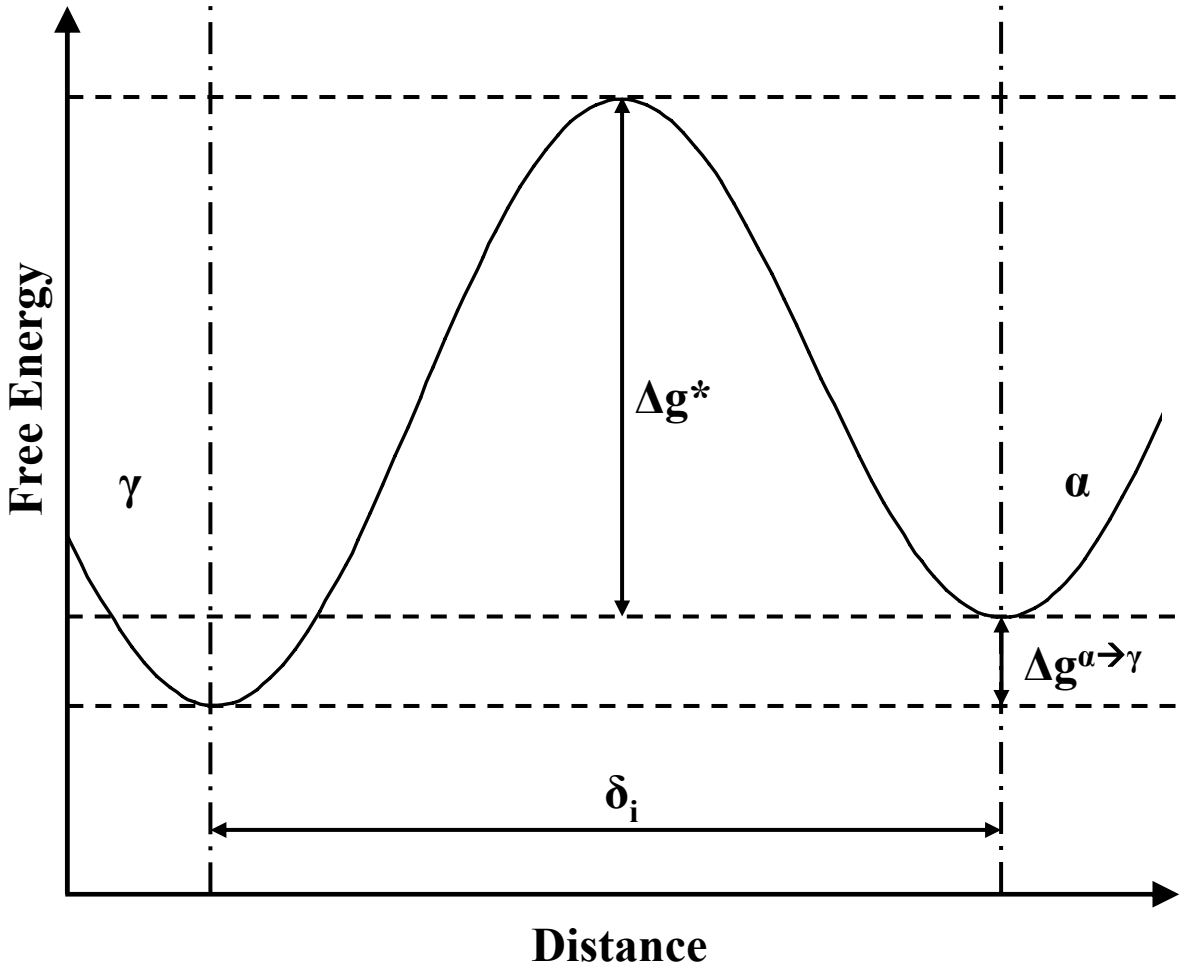

- $R_{net} = R_{forward} - R_{reverse}$
- Thermally-activated migration (Eyring):

$$\dot{R} = S\nu \exp\left(\frac{-\Delta g^*}{kT}\right)\left(1 - \exp\left(\frac{-\Delta g^{\alpha\to\gamma}}{kT}\right)\right)$$

- If $\Delta g^{\alpha\to\gamma} << kT$, then we can approximate:

$$1 - \exp\left(\frac{-\Delta g^{\alpha\to\gamma}}{kT}\right) = 1 - \left(1 + \frac{-\Delta g^{\alpha\to\gamma}}{kT}\right) = \frac{\Delta g^{\alpha\to\gamma}}{kT}$$

- Velocity is related to this rate by:

$$\dot{v} = \frac{\delta_i \dot{R}}{S}$$

- And we get the previous expression for velocity:

$$\dot{v} = \frac{\delta_i \nu}{kT} \exp\left(\frac{\Delta s^*}{k}\right) \exp\left(\frac{-\Delta h^*}{kT}\right) \Delta g^{\alpha\to\gamma}$$

Driving Force for DCG and ICG in Fe-C

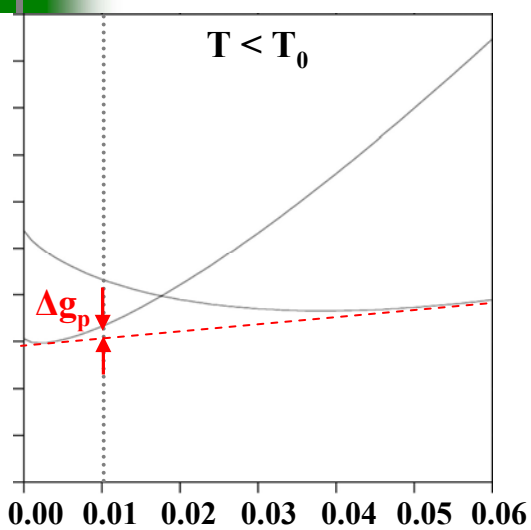

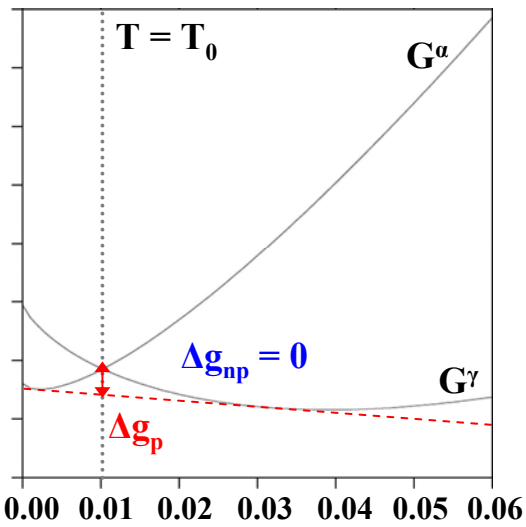

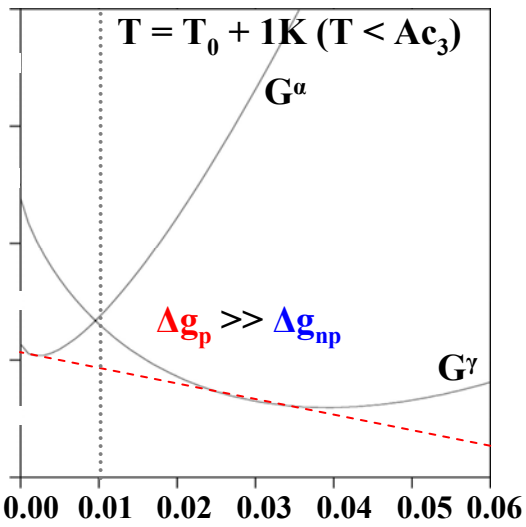

G ↑
(1 tick mark = 10 J/mol)

Wt% C →

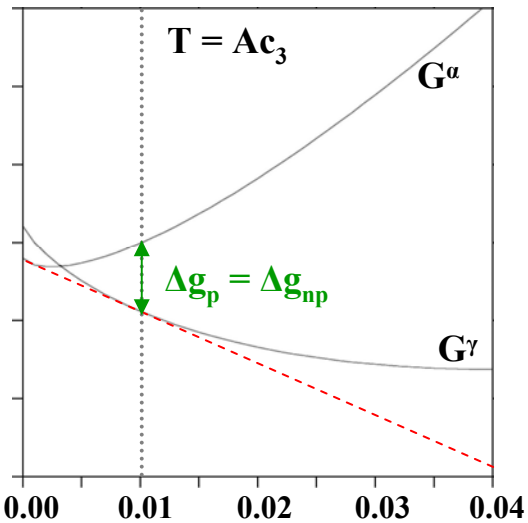

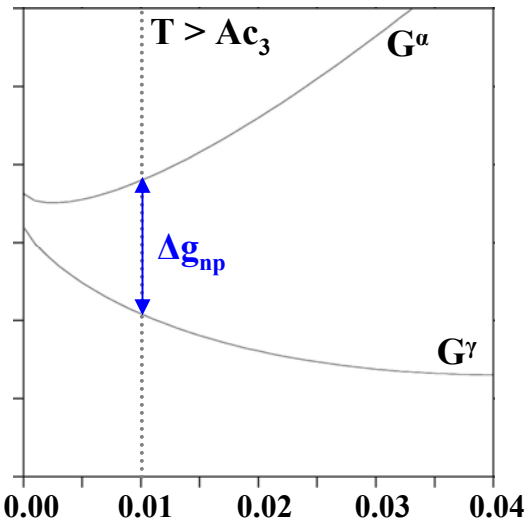

Normalized Fe-C: Non-Isothermal Analysis

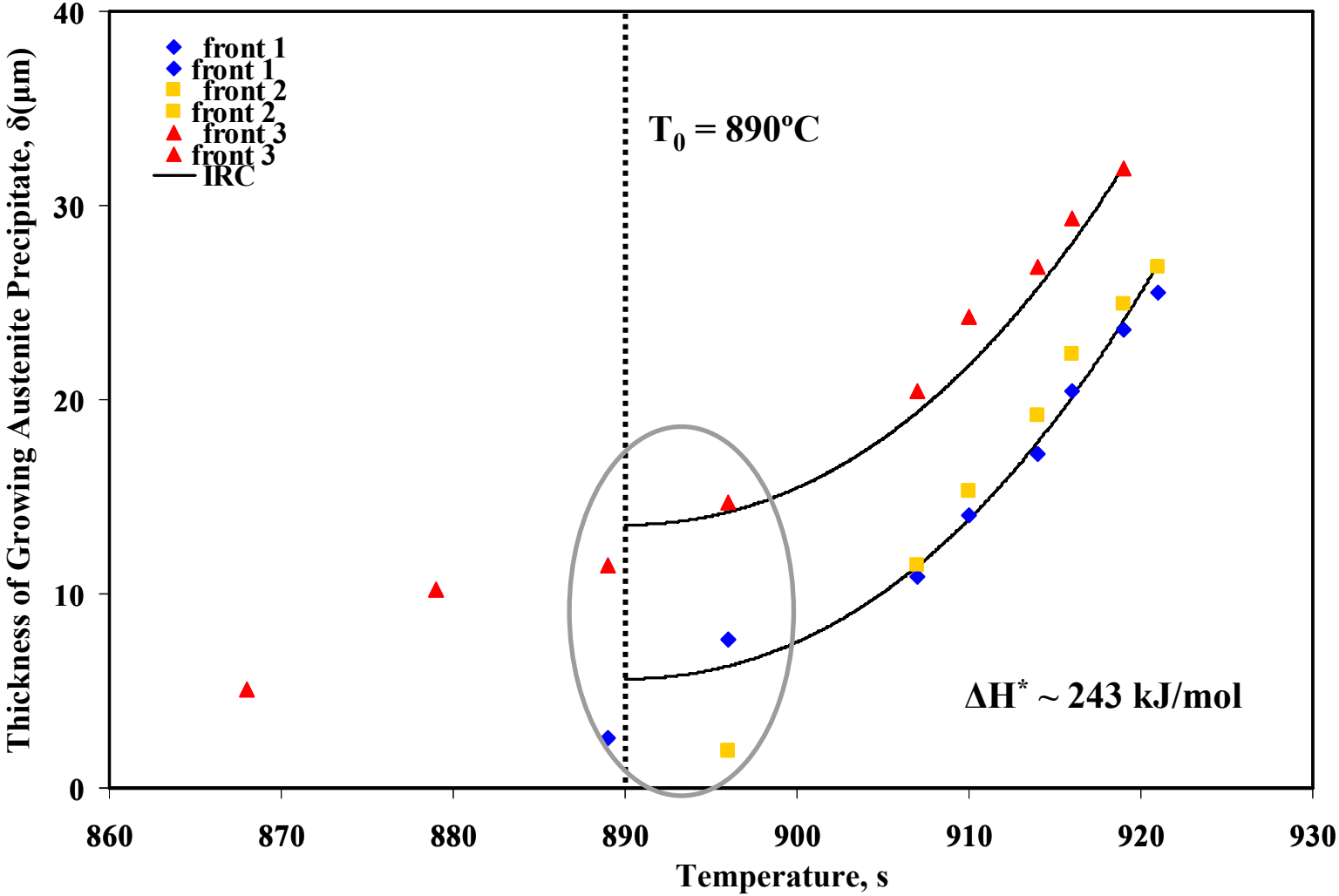

Normalized Fe-C, 900°C Isothermal Analysis

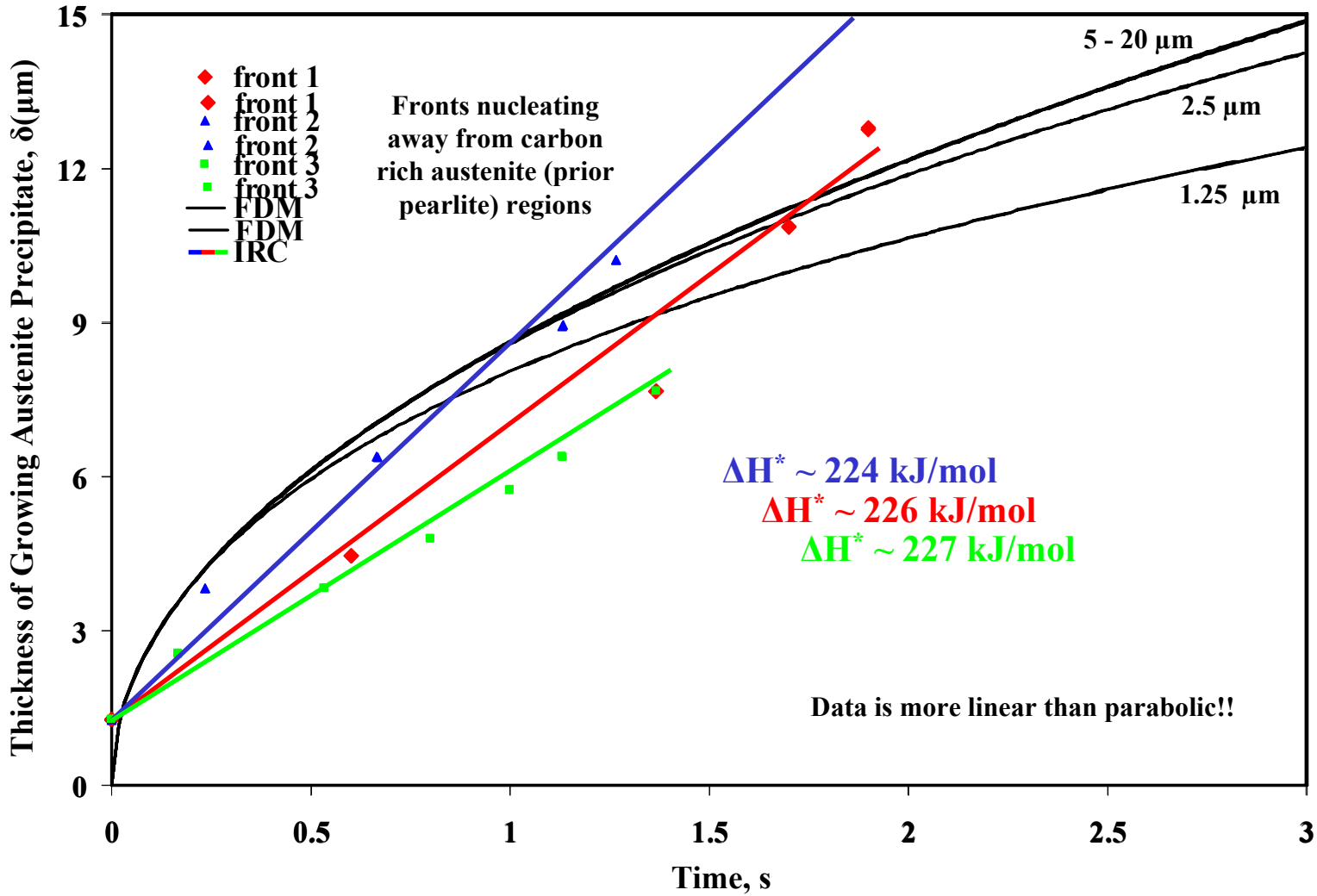

Driving Force for DCG and ICG

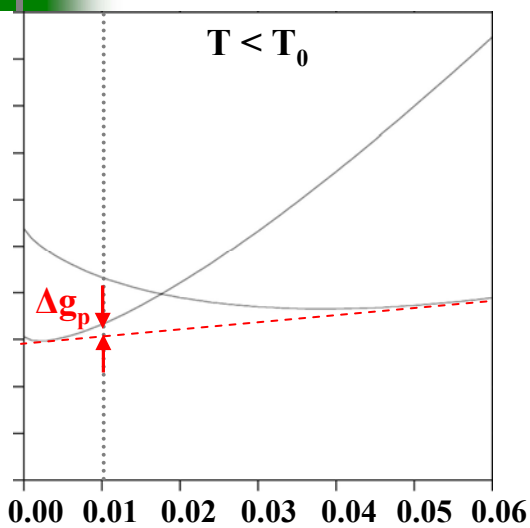

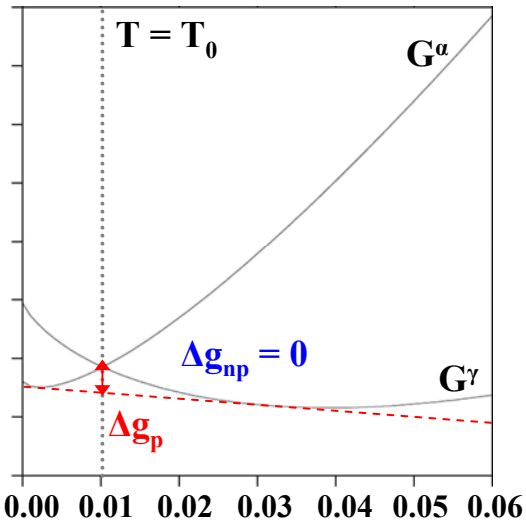

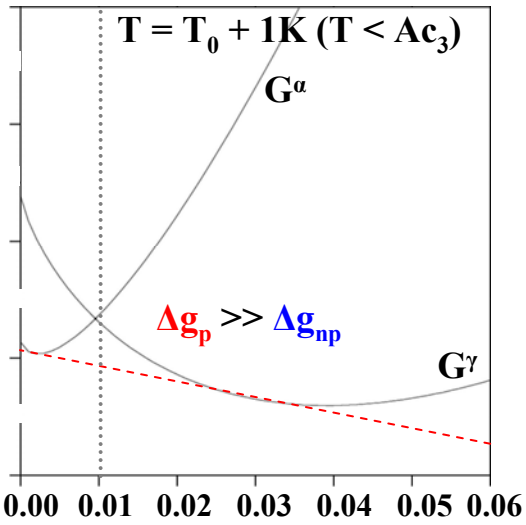

G ↑
(1 tick mark = 10 J/mol)

Wt% C →

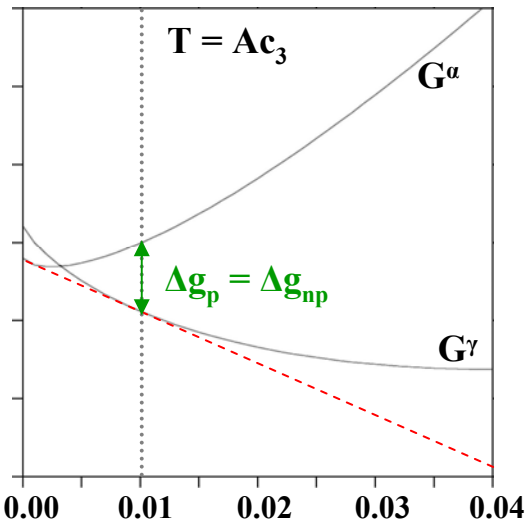

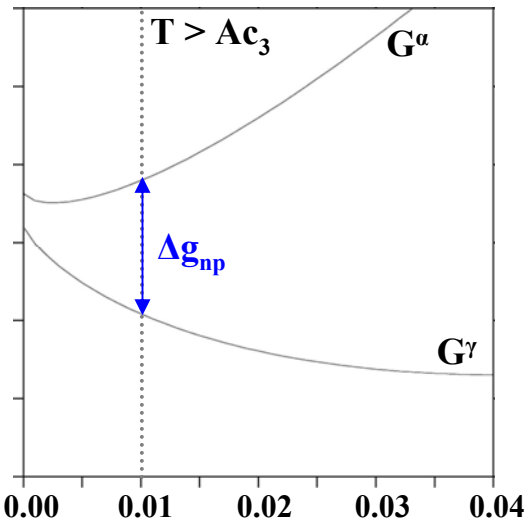

Summary: Transition from ICG to DCG

- What we know:
  - Diffusion model predicts faster boundary migration than ICG at highest intercritical temperatures
    - Combination of increasingly small difference between equilibrium interface compositions and mass conservation at the interface
    - Increasing diffusion coefficients
  - Interface reaction becomes rate controlling at some point near T_0
    - Could be above or below, but must be below Ac_3
    - Driving force resulting from partitioned interface is much greater than for partitionless just above T_0
    - Partitioned and partitionless driving force converge as temperature approaches Ac_3
  - Partitionless, ICG (e.g. massive) must occur above Ac_3

Annealed (Coarse-grained) Fe-C

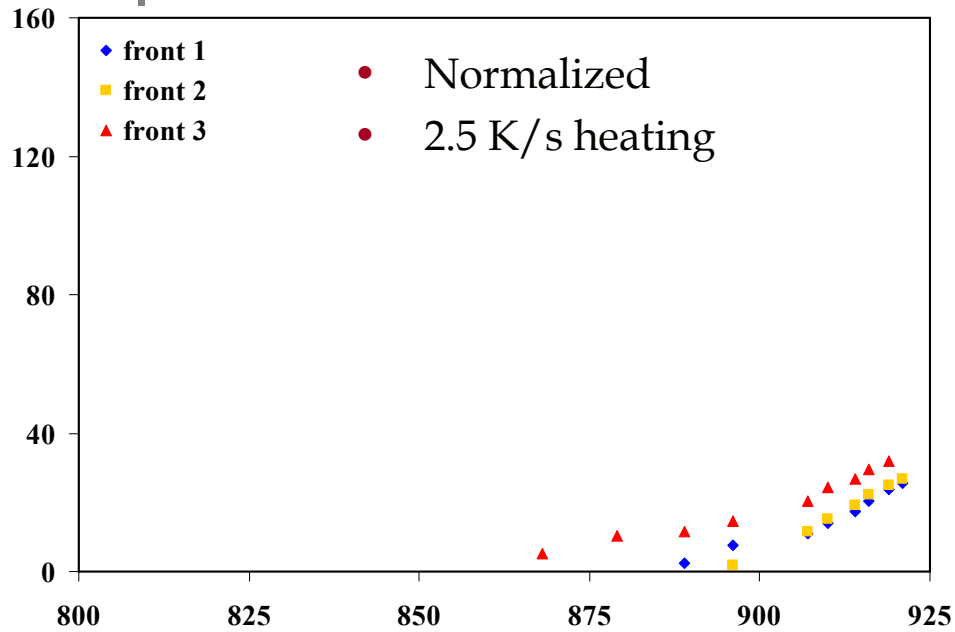

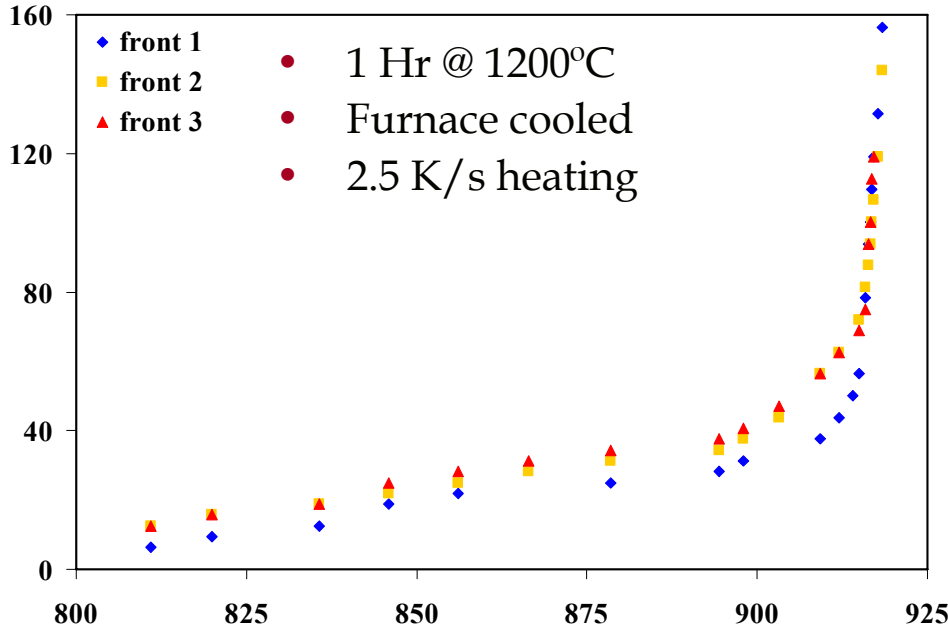

- Furnace cooled: Carbon content may be much lower in ferrite than in normalized (air cooled) samples due to extremely slow cooling in furnace (8-12 hrs)
- Indicates strong effect of carbon on interface mobility

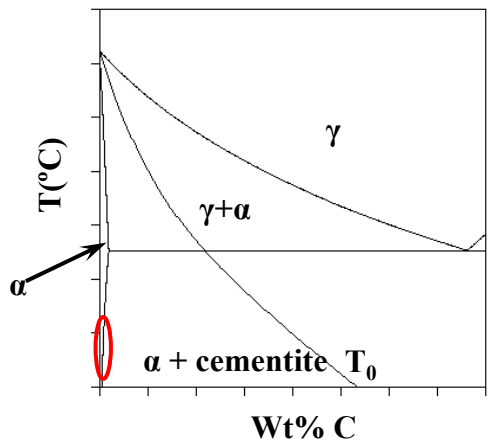

Annealed (Coarse-grained) Fe-C

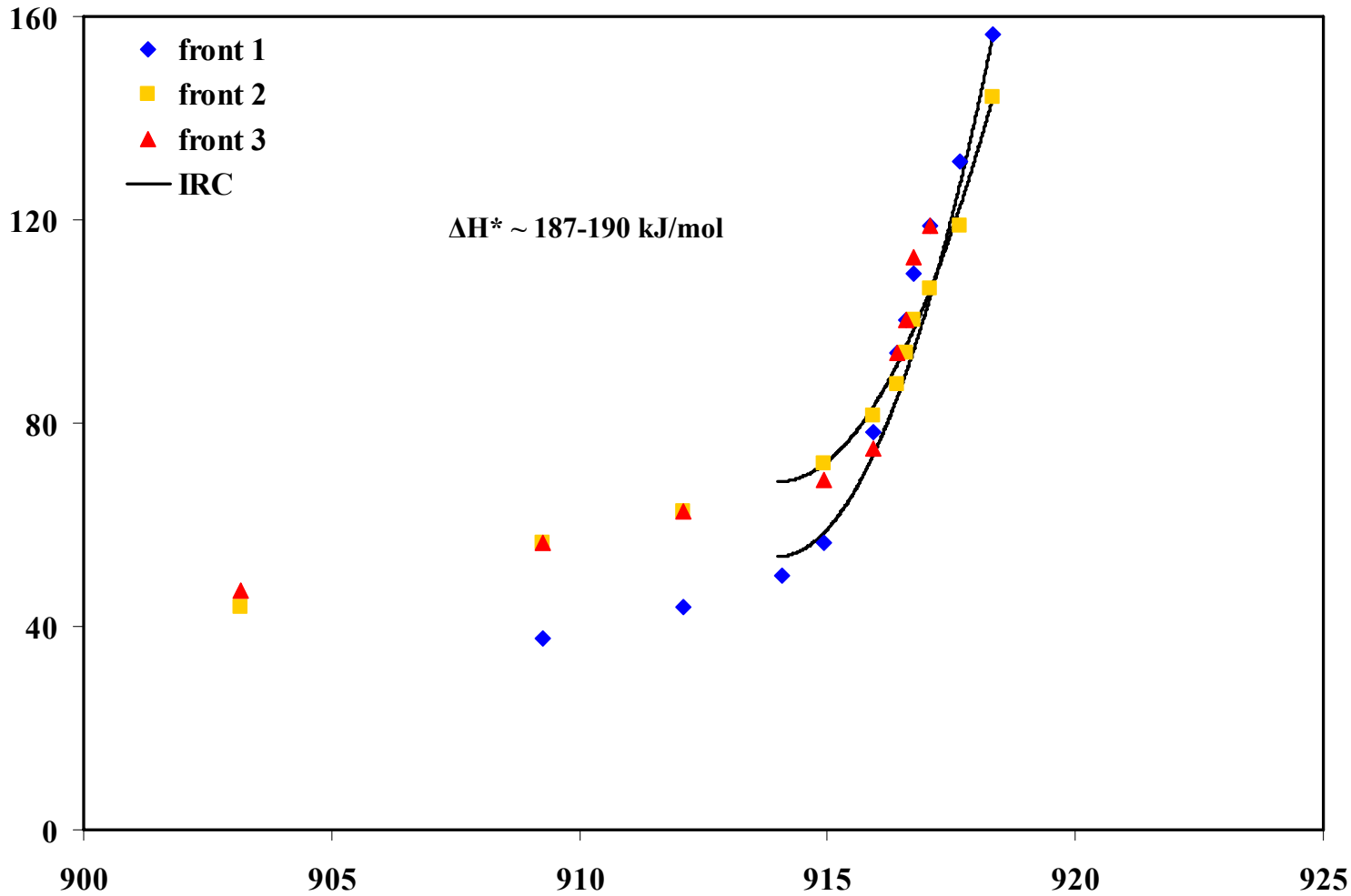

Annealed Fe-C: Rapid cycling

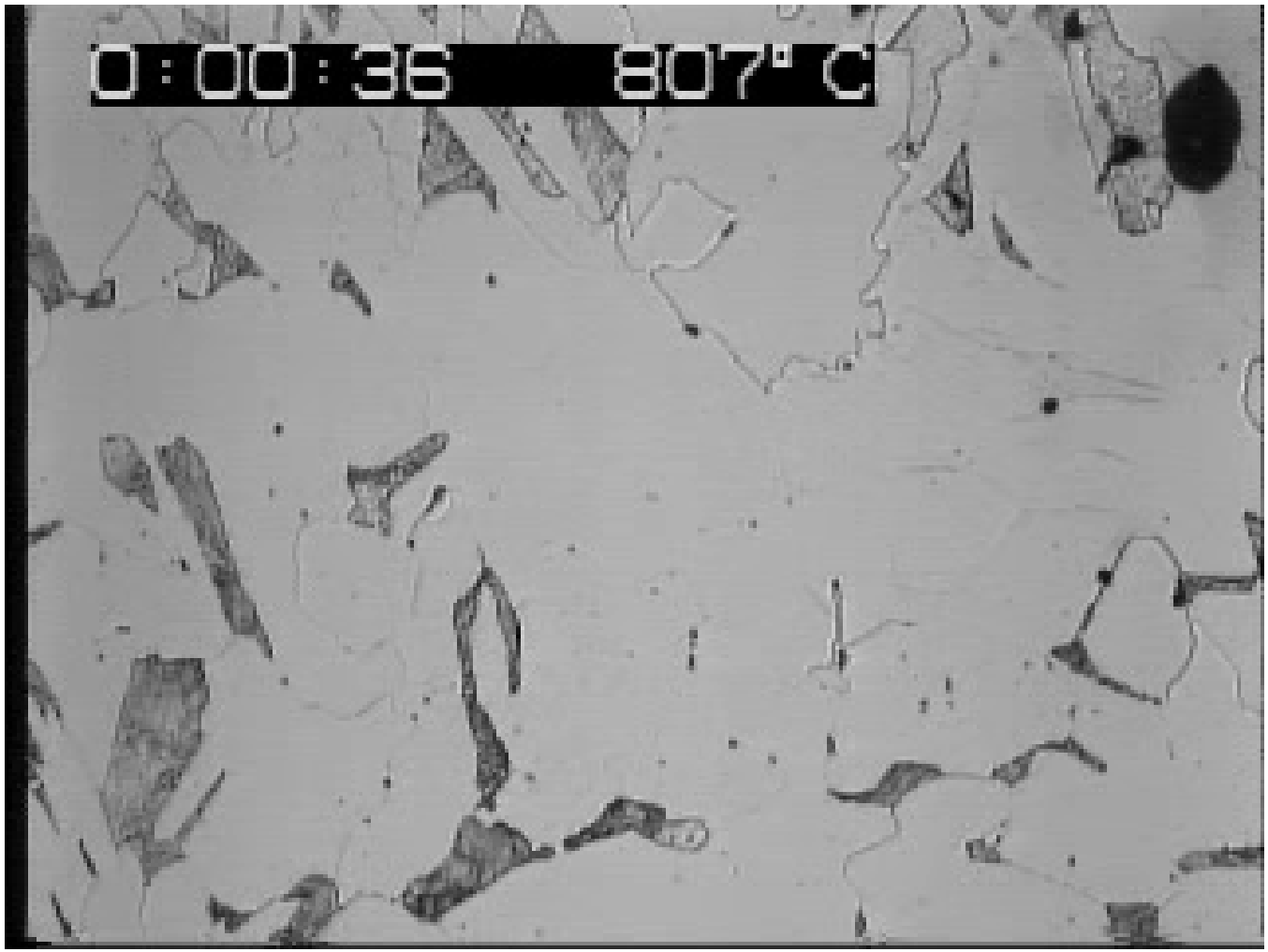

- 20 K/s Heating, He quench

~120 µm

Compare: Intercritical Annealing of Alloy Steel

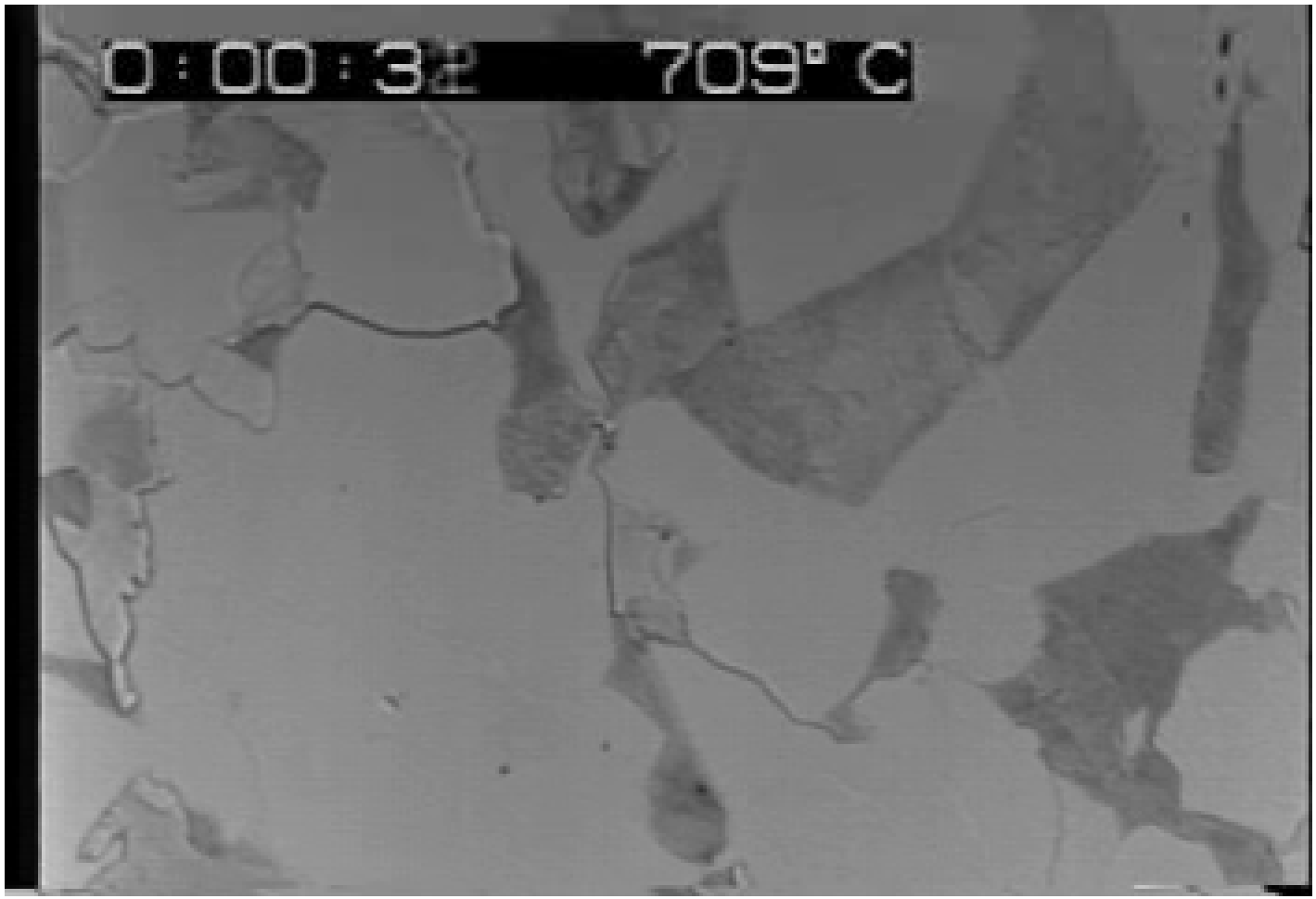

~30 µm

4118, 790ºC isothermal hold, Quench in He gas

Summary: Alloying Effects on Mobility

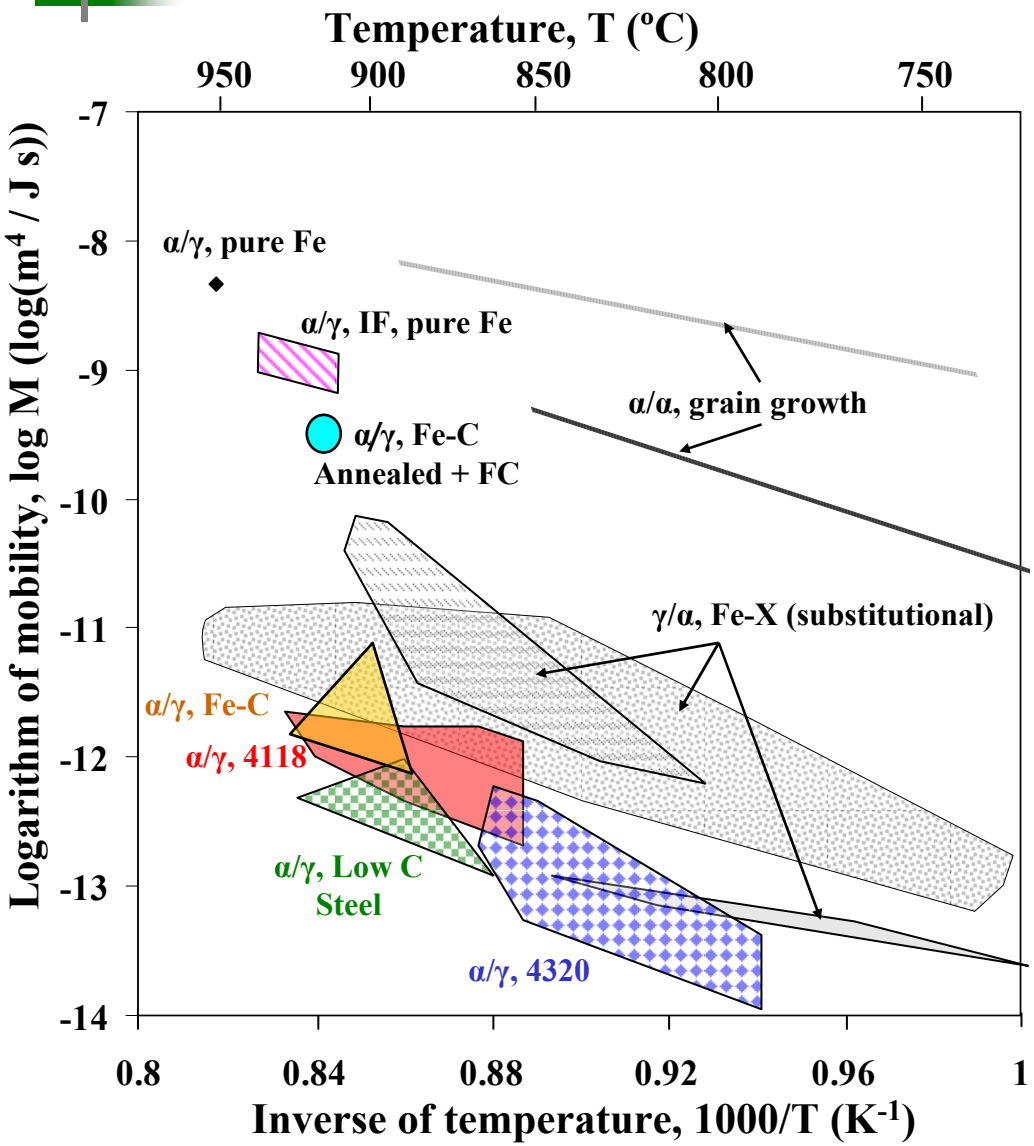

$$\dot{\nu} = \left(\frac{\delta\nu}{kT}\right)\exp\left(\frac{\Delta S^*}{k}\right)\exp\left(\frac{\Delta H^*}{kT}\right)\Delta g^{\alpha\to\gamma}$$

$$M = \frac{\nu \cdot V_m}{\Delta g \cdot N_A}$$

Investigation Details	Year
Speich and Szirmae; pure Fe, laser heating	1968
Ivanov and Osipov; pure Fe, anneal/section/polish	1961
Hu, pure Fe; anneal/section/polish	1974
Vooijs *et al.*, Fe-C, Cr, DTA	2001
Wits *et al.*, Fe-C-Co,Cu,Mn,Al,Cr, Dilatometry	2000
Krielaart and Van der Zwaag, Fe-Mn, DTA	1998

- Normalized Fe-C, Alloy Steels: activation enthalpy ~ bulk diffusion (250 kJ/mol)
- Pure/IF: activation enthalpy ~ grain boundary diffusion (160 kJ/mol)
- Impurity threshold → drastic change in mobility? Capdevelia *et al.*, 2003 (ferrite grain boundaries)

Acknowledgements

- Prof. Seetharaman
- National Science Foundation, CAREER grant DMR 0348818
- Center for Iron and Steelmaking Research
- Dr. Buddy Damm and The Timken Corporation
- Madhavi Ganapathiraju
- Madeline Lesko
- All of my fellow group members (past and present)

Discussion Topics

$$\dot{\nu} = \frac{\delta_i \nu}{kT} \exp\left(\frac{\Delta s^*}{k}\right) \exp\left(\frac{-\Delta h^*}{kT}\right) \Delta g^{\alpha \to \gamma}$$

- What is Δs*?
  - Can we use statistical mechanics to determine?
- Is there a single activated state, or is there an additional potential well inside the interface?
- Is it more likely that variations in Δh* or Δs* cause the large mobility differences?
  - How do the alloying elements effect these values?
- Coupling the LRD model with ICG model
  - Transport of carbon to interface determines driving force, which in turn determines the migration rate

Summary: Materials

Sample	C	Mn	Cr	Ni	Mo	Si
IF-A	0.004	0.05	0.03	0.03	0.005	0.03
IF-B	0.006	0.06	0.03	0.03	0.006	0.02
Fe-C	0.14	0.01	0.01	0.01	0.01	0.01
Low C	0.037	0.19	0.046	0.034	0.01	0.08
4118	0.20	0.87	0.56	0.10	0.09	0.31
4320	0.20	0.54	0.47	1.74	0.21	0.21

Sample	Al	Ti	Cu	N	S	P
IF-A	0.05	0.06	0.10	0.006	0.003	0.01
IF-B	0.04	0.06	0.08	0.006	0.006	0.01
Fe-C	0.009	0.001	0.01	0.0008	0.01	0.002
Low C	0.024	0.002	0.174	.009	0.003	0.008
4118	0.042	0.002	0.22	-	0.030	0.010
4320	0.021	0.001	0.15	-	0.018	0.006

(Steel compositions are given in wt%)

Initial Microstructures

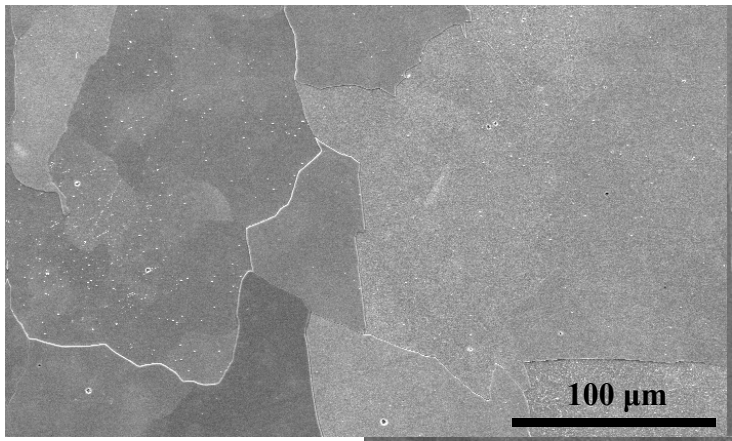

IF-A

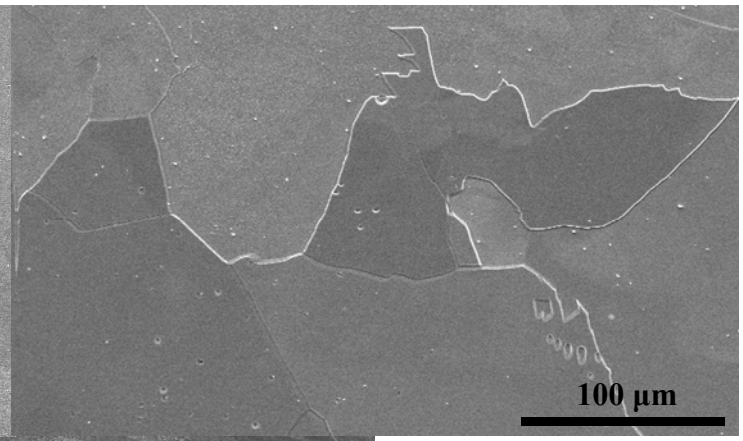

IF-B

Pure Fe
(99.995%)

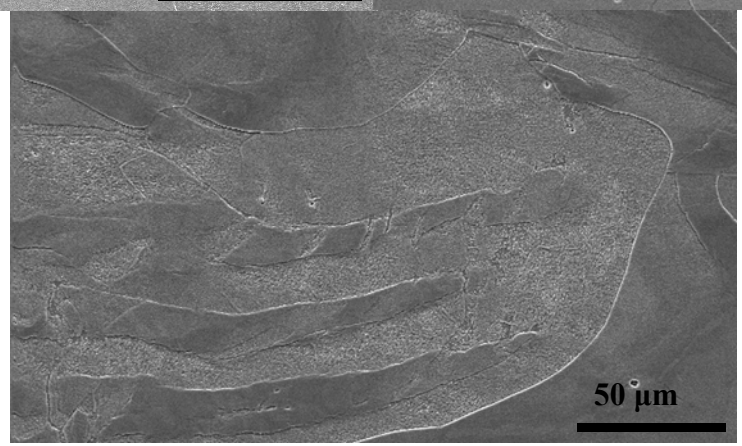

- Pure iron, IF steels
  - Ferrite grains only
  - IF contains some non-metallic inclusions: nitrides, oxides

4118

4320

Initial Microstructures

Fe-C

Low-C

4118

4320

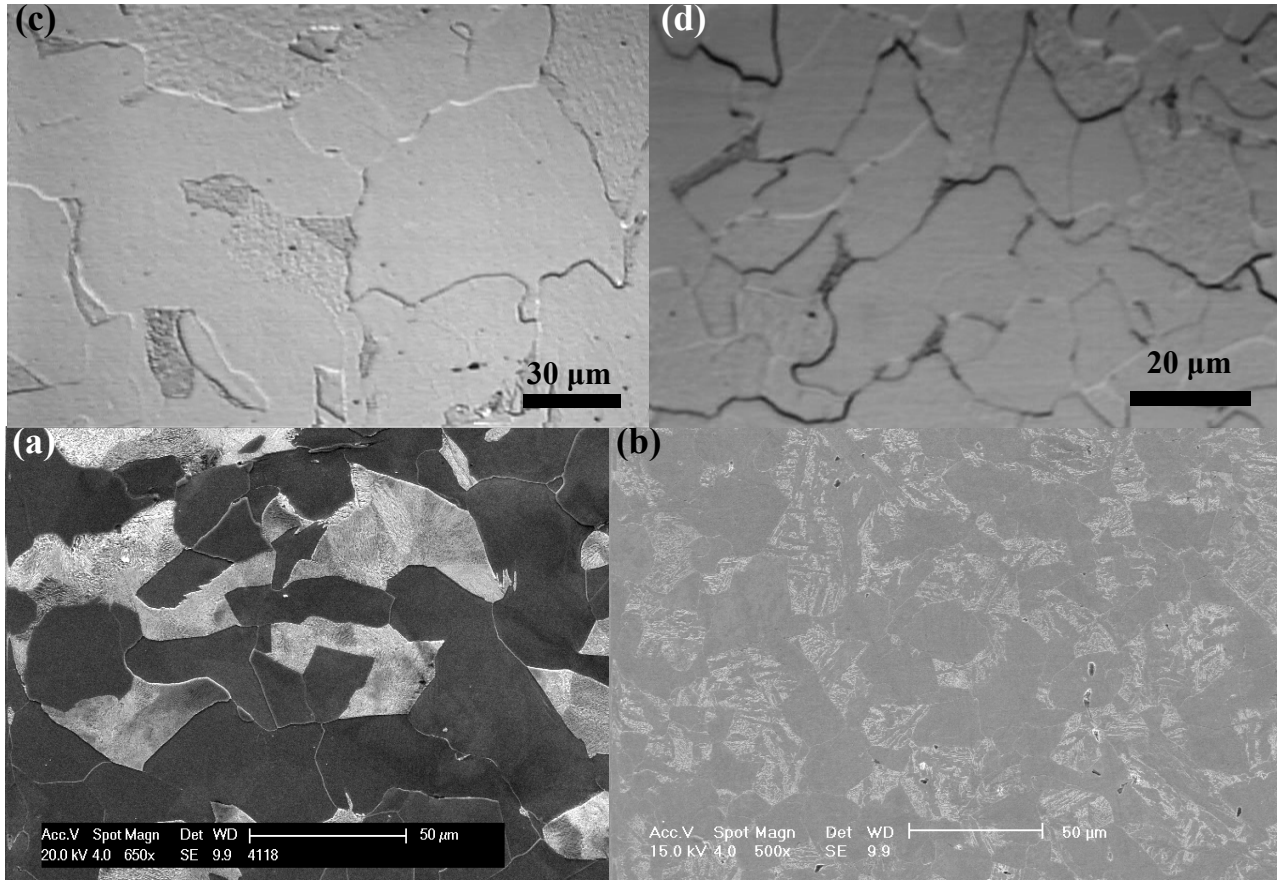

- Fe-C, Alloy steels
  - Mixed microstructure
  - Fe-C, Low C, and 4118 steels contain ferrite + pearlite
  - 4320 Steel contains ferrite + bainite

What can we Observe?

- Solidification
  - Peritectic, Eutectic
- Grain Growth
- Solid-State Phase Transformations
  - Austenite Decomposition
    - Into ferrite, pearite, bainite, martensite
  - Austenite Formation
    - From low or high temperature ferrite

Interpreting CLSM Observations

- Distinguish the concurrently occurring phenomena
  - (i) surface relief due to phase transformation

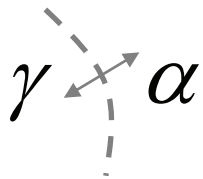

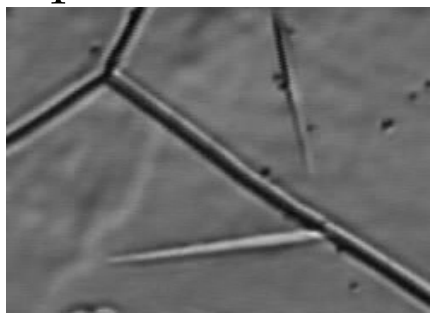

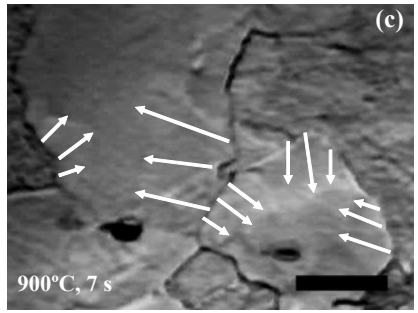

  - (ii) smoothening of relief and grooves due to surface diffusion
  - (iii) grain boundary grooving and migration

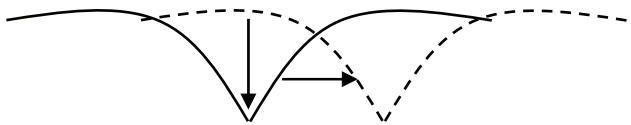

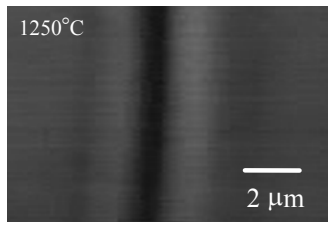

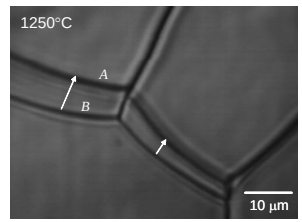

  - (iv) reactions with atmosphere

(Images courtesy of Casper Thorning, CMU)

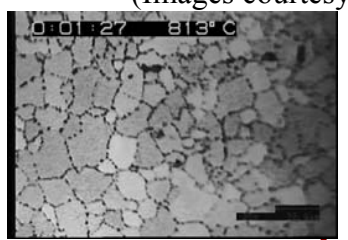

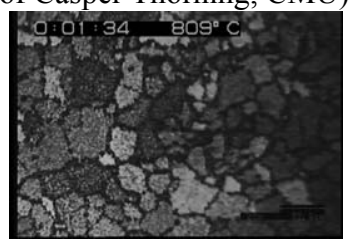

Massive Transformation in Mixed Microstructure

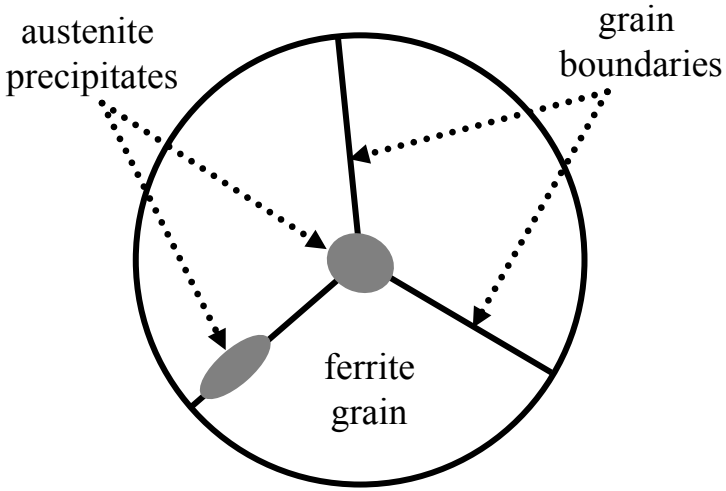

- In iron and fully ferritic steels, the microstructure is homogenous during austenitization

- Iron-carbon alloys do not have a uniform structure; however:
  - If ferrite grains are heated rapidly enough, the austenite may form in similar locations (red) as in the fully ferritic structure
  - These austenite precipitates are 'unaware' of non-homogeneous structure
  - Would be the case for any partitionless phase change in ferrite regions

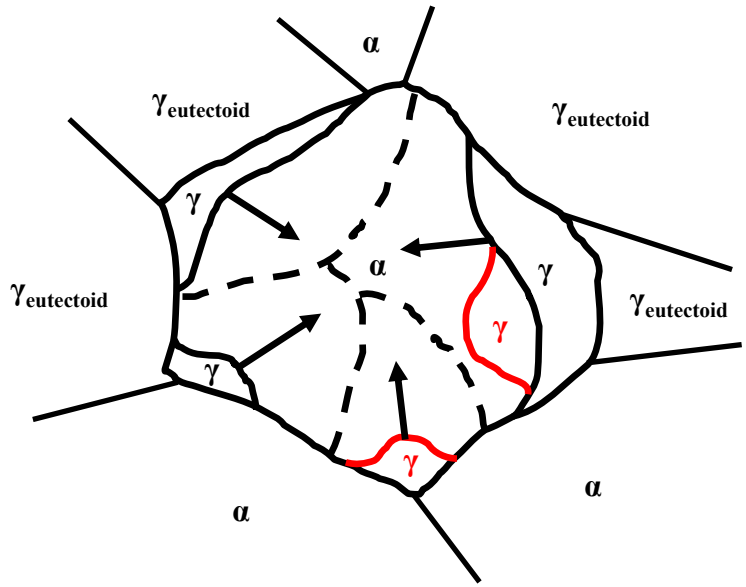

Observations: IF Steel

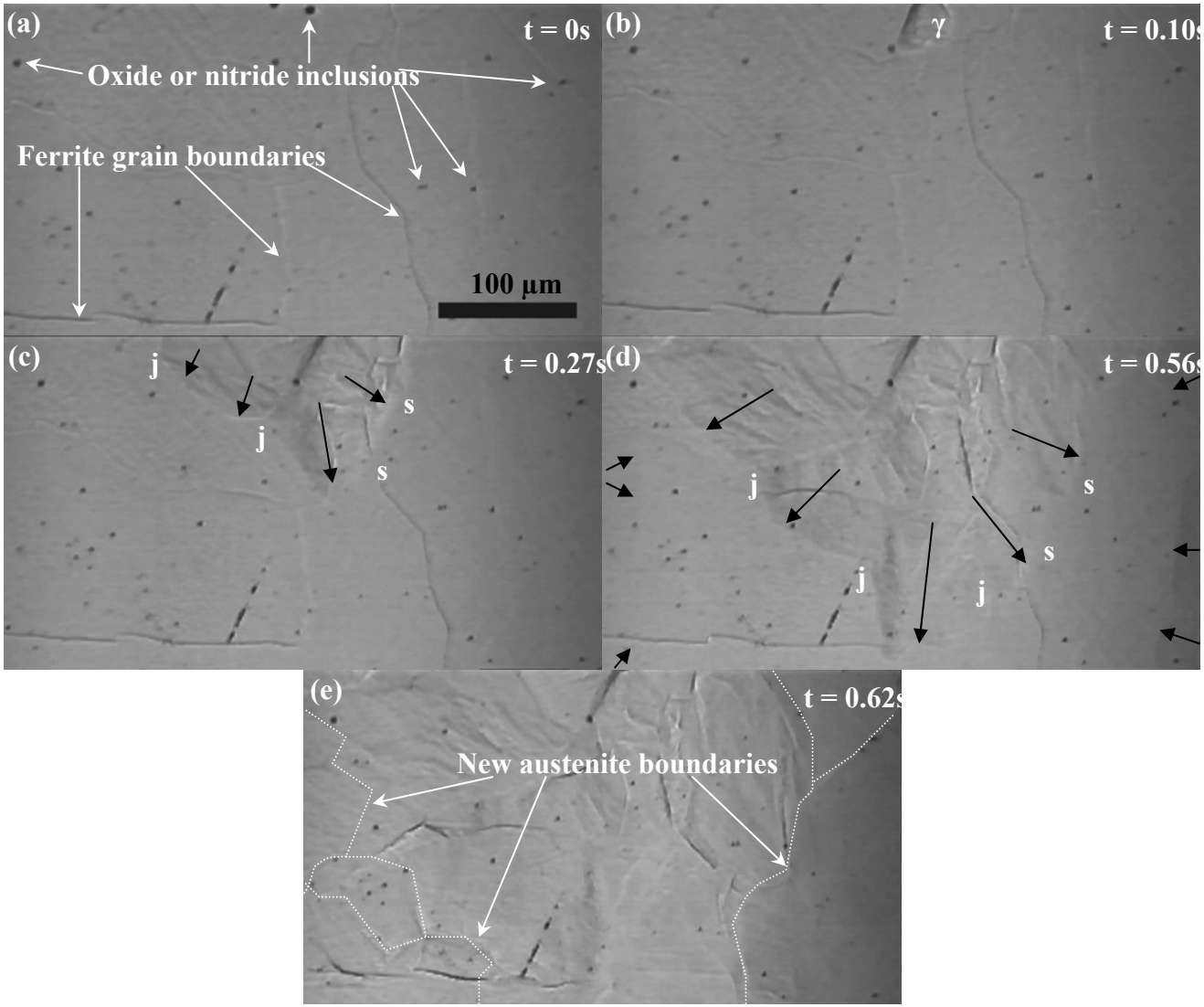

IF Steel Inclusions

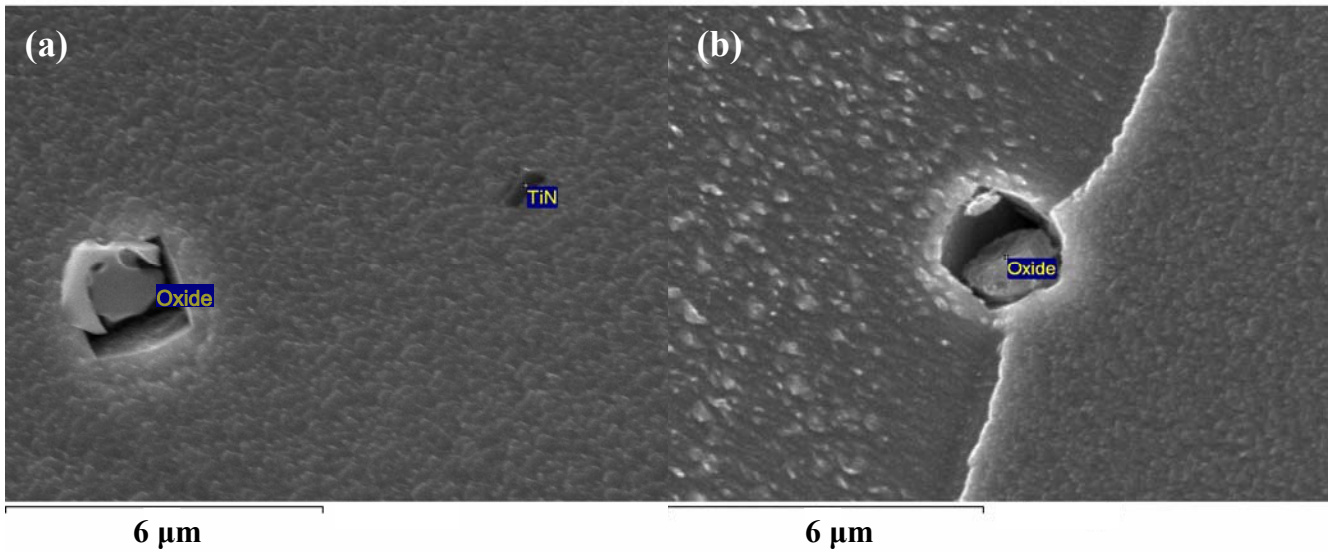

Particle #	Type	Diameter (µm)	Sample	Location	Figure
6	Oxide	2.5	IF-B	Matrix	5.2a
7	Oxide	1.75	IF-B	GB	5.2b
9	Nitride	1	IF-B	Matrix	5.2a

Particle#	%Ti	%Ca	%Al	%Mg	%Fe	%Mo	%O	%N
6	3.17	-	22.40	6.23	-	-	68.19	-
7	2.76	2.81	16.29	3.04	-	-	75.09	-
9	57.65	-	-	-	-	-	-	42.35